SIDELOBE SUPPRESSION FOR OFDM BASED COGNITIVE RADIOS IN DYNAMIC SPECTRUM ACCESS NETWORKS

Srikanth Pagadarai
B.Tech.(Electronics & Communications Engineering, Jawaharlal Nehru Technological University)

Submitted to the Department of Electrical Engineering & Computer Science and the Faculty of the Graduate School of the University of Kansas in partial fulfillment of the requirements for the degree of Master's of Science

Thesis Committee:

Dr. Alexander M. Wyglinski: Chairperson

Dr. Gary J. Minden

Dr. Erik S. Perrins

Date Defended: 08/23/07

The Thesis Committee for Srikanth Pagadarai certifies
that this is the approved version of the following thesis:

SIDELOBE SUPPRESSION FOR OFDM BASED COGNITIVE RADIOS IN DYNAMIC SPECTRUM ACCESS NETWORKS

Committee:

Chairperson

Date Approved: 08/23/07

Abstract

As the demand for sophisticated wireless mobile applications incorporating efficient modulation techniques is ever increasing, more bandwidth is needed to support these applications. However, bandwidth is a limited resource. Also, as the existing spectrum allocation policies of the Federal Communications Commission (FCC) allow spectrum access to licensed users only, it has been proven by various spectrum measurement campaigns that, the current licensed spectrum usage across time and frequency is inefficient. Therefore, in order for the unlicensed users to access the unused portions of the licensed spectrum, the concept of "spectrum pooling" has been proposed.

Spectrum pooling is based on dynamic spectrum access (DSA), wherein the secondary user decides on whether or not a particular frequency band is currently being used and transmits the signal in that unused licensed band, while ensuring that the system performance of the primary as well as the secondary is not impacted. Thus, coexistence of the primary and the secondary users is an important criterion that makes DSA a feasible solution for efficient spectrum usage. This thesis investigates an important problem concerning the coexistence of the primary and the secondary users.

Orthogonal frequency division multiplexing (OFDM) has proven to be the prime candidate for spectrum pooling based wireless transmission systems as it can support high data rates and is robust to channel impairments. Even though the secondary transmissions help in improving the spectral efficiency by transmitting in the spectral white spaces left unused by the primary users, the large sidelobes resulting from the use of OFDM result in high out-of-band (OOB) radiation. Thus, the coexistence of the primary and the secondary users in the form of spectrum sharing is dependant on the suppression of the interference from the rental systems to the legacy systems. This thesis presents two novel techniques to suppress the

OOB interference from the secondary user to the primary user, while not affecting the other system parameters of the secondary user by a great deal.

To my parents and my brother

Acknowledgements

I would like to express my deepest gratitude to my advisor Dr. Alexander M. Wyglinski for giving me an opportunity to work with him. I thank him for his excellent guidance and continual support during the course of my Master's at KU. Working with him has been a wonderful productive experience. His valuable advice and the wide knowledge that he shared during my association with his Signals Modulation and Routing (SMART) group has been invaluable.

I would like to thank Dr. Gary J. Minden and Dr. Erik S. Perrins for agreeing to be on my committee. Their suggestions and comments with regards to my thesis have helped me improve my work. Special thanks to former Ph.D student, Dr. Rakesh Rajbanshi, whose guidance has been an immense boost to my research. Working with him has been truly inspiring.

During the course of my graduate studies at KU, I have had the pleasure of meeting many students, who have helped me directly or indirectly in completing my studies and have made my Master's a rewarding experience. I owe my thanks to them. In particular, I would like to thank SMART group members, Udaya Kiran Tadikonda, Shilpa Sirikonda, Satish Kumar Chilakala, Padmaja Yatham, Vinay Kumar Muralidharan, and Bharatwajan Raman. I would also like to thank Michael Hulet, Wesley Mason, Paula Conlin and other staff members at ITTC, KU. I thank my close friends during my under-graduation, who have become an inseparable part of my life.

I am deeply indebted to my parents and my brother who have been a constant source of support and love throughout this degree and my life. Thank you for everything.

Contents

Acceptance Page **i**

Abstract **ii**

Acknowledgements **v**

1 Introduction **1**

1.1 Research Motivation 1

1.2 Research Objective 4

1.3 Current State-of-the-art 5

1.4 Thesis Contributions 7

1.5 Thesis Organization 8

2 OFDM-based Cognitive Radio **9**

2.1 A Spectrum Pooling-based Cognitive Radio for Flexible Wireless Communications 9

2.2 An Overview of Orthogonal Frequency Division Multiplexing (OFDM) 12

2.2.1 Introduction 12

2.2.2 A general schematic of an OFDM-based cognitive radio transceiver 15

2.2.3 Channel model 20

2.2.4 Synchronization in OFDM-based transceiver systems . . . 22

2.2.5 Peak-to-average power ratio 24

3 Out-of-band Interference Problem in OFDM **27**

3.1 Interference to the Legacy System 28

3.1.1 Windowing: A simple countermeasure to the interference from rental system 31
3.1.2 Insertion of guard bands: Another simple technique for interference suppression 33
3.2 A brief summary of the existing Sidelobe Suppression Techniques 36

4 Proposed Techniques for Sidelobe Suppression 39
4.1 Proposed Sidelobe Suppression using Cancellation Carriers 39
4.1.1 Schematic of an OFDM transceiver employing cancellation carriers for sidelobe suppression 40
4.1.2 Proposed sidelobe suppression technique 41
4.1.3 Simulation Results 44
4.2 Proposed Sidelobe Suppression by Constellation Expansion 53
4.2.1 Schematic of an OFDM transceiver employing constellation expansion for sidelobe suppression 54
4.2.2 Proposed CE-based sidelobe suppression technique 55
4.2.3 Simulation Results 60

5 Conclusion 71
5.1 Future Work 72

References 74

List of Figures

1.1 Spectrum occupancy measurements from 9 kHz to 1 GHz (8/31/2005, Lawrence, KS, USA). 2

2.1 An illustration of the conventional and orthogonal FDM techniques 13
2.2 OFDM signal spectrum of a N=8 subcarrier OFDM transceiver using DFT 14
2.3 A general schematic of an OFDM-based cognitive radio transceiver 16
2.4 An illustration showing the time domain waveforms of a N=8 subcarrier OFDM transceiver system that are summed to create parallel data signals 18
2.5 An illustration showing the time domain composite OFDM symbol of the N=8 subcarrier OFDM transceiver system 19
2.6 An illustration showing the effect of ICI to the desired OFDM symbol due to frequency offset 22
2.7 An illustration showing the time domain waveforms of a N=16 subcarrier BPSK-OFDM transceiver system 25

3.1 An illustration of the interference due to one OFDM-modulated carrier 29
3.2 An illustration of the interference in a BPSK-OFDM system with N=16 subcarriers 31
3.3 Structure of the temporal OFDM signal using a raised cosine window 32
3.4 Impact of rolloff factor on the PSD of the rental system signal. . . 33
3.5 An illustration of the guard band technique for sidelobe suppression 34
3.6 Interference suppression in a BPSK-OFDM system with N=64 subcarriers by inserting guard bands 35

4.1 Schematic of an OFDM-based cognitive radio transceiver employing the proposed sidelobe suppression technique. 40
4.2 An illustration of the sidelobe suppression using the proposed technique. 44
4.3 Averaged BPSK-OFDM spectrum with and without inserting cancellation carriers(CCs). 46
4.4 Averaged QPSK-OFDM spectrum with and without inserting cancellation carriers(CCs). 47
4.5 Complementary cumulative distribution function (CCDF) with and without inserting cancellation carriers (CCs). 48
4.6 Complementary cumulative distribution function (CCDF) with and without inserting cancellation carriers (CCs) in a BPSK-OFDM system. 50
4.7 Complementary cumulative distribution function (CCDF) with and without inserting cancellation carriers (CCs) in a QPSK-OFDM system. 51
4.8 An example showing the application of the proposed sidelobe suppression algorithm in a spectrum sharing scenario. 53
4.9 Effect of the CCs on the PAPR of N=64 subcarrier QPSK-OFDM system 54
4.10 Schematic of an OFDM-based cognitive radio transceiver employing the proposed CE-based sidelobe suppression technique. 56
4.11 Two ways of mapping symbols from BPSK constellation to QPSK 57
4.12 Two ways of mapping symbols from QPSK constellation to 8PSK 58
4.13 An iterative algorithm for symbol selection using constellation expansion 59
4.14 Sidelobe levels of a BPSK-OFDM system with and without constellation expansion 62
4.15 Sidelobe levels of a QPSK-OFDM system with and without constellation expansion 63
4.16 CCDF of sidelobe power for QPSK-modulated OFDM and its expanded 8-PSK modulated OFDM for different number of iterations 64
4.17 CCDFs of sidelobe power for BPSK-modulated OFDM and its expanded QPSK modulated OFDM for different mappings 65

4.18 Sidelobe levels of a BPSK-OFDM system with and without constellation expansion 66
4.19 Sidelobe levels of a QPSK-OFDM system with and without constellation expansion 67
4.20 An example showing the application of the proposed sidelobe suppression algorithm in a spectrum sharing scenario. 68
4.21 BER of a N=16 subcarrier QPSK-modulated OFDM and its expanded 8-PSK modulated OFDM 69
4.22 PAPR plot of a N=16 subcarrier QPSK-modulated OFDM and its expanded 8-PSK modulated OFDM 70

Chapter 1

Introduction

1.1 Research Motivation

With the increase in the demand for radio frequency (RF) spectrum, and with the non-availability of "prime" spectrum, the expansion of the existing services or the allocation of spectrum for additional services was an important technical challenge identified by the Federal Communications Commission (FCC). The traditional spectrum allocation techniques rely on segmenting the available spectrum and assigning the fixed blocks to the licensed users. In such a spectrum allocation scenario, unlicensed users are not permitted to access the already licensed bands since strict regulations are imposed on their access. As a result of the prohibition on the unlicensed access to licensed spectrum, heavily populated and highly interference-prone frequency bands have to be accessed. Clearly, this results in reduced system performance.

Moreover, measurement campaigns have shown that such an allocation causes a waste of the spectrum both in frequency and time [1]. Figure 1.1 shows a measurement campaign conducted at the Information Technology and Telecom-

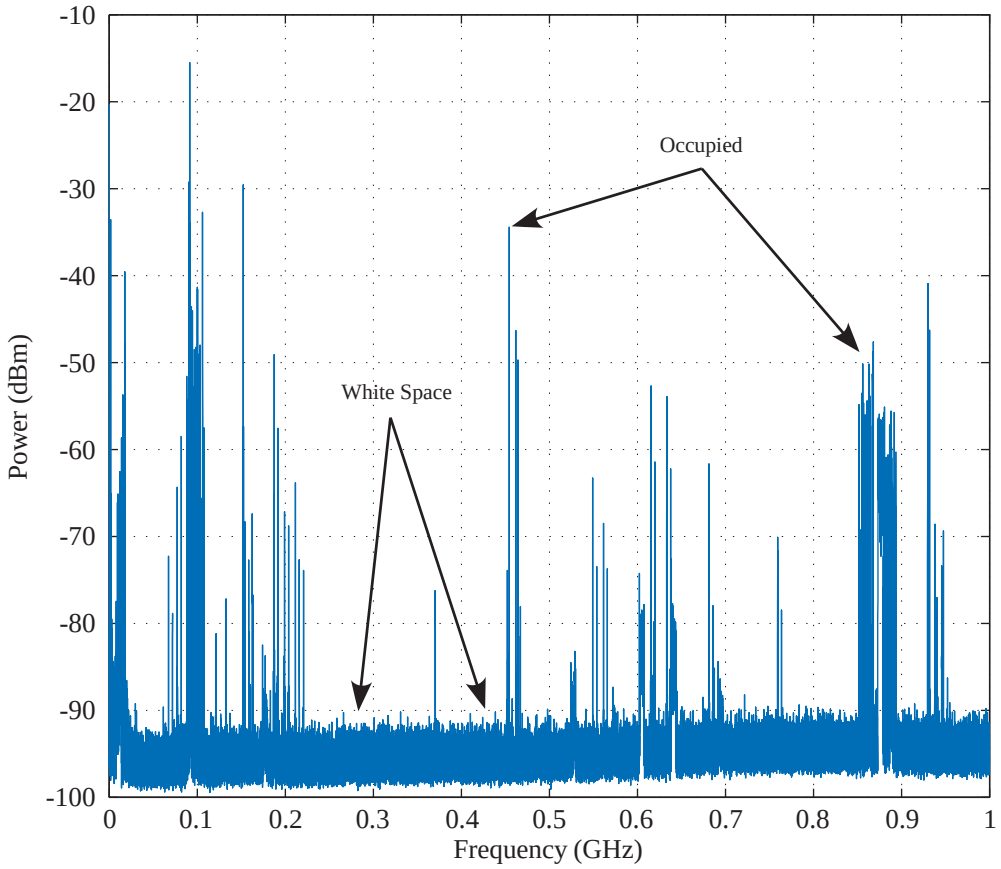

Figure 1.1. Spectrum occupancy measurements from 9 kHz to 1 GHz (8/31/2005, Lawrence, KS, USA).

munications Center (ITTC) on 8/31/2005 [2]. The spectral occupancy from 9 kHz to 1 GHz is shown. From this figure, it is observed that there are several spectral white spaces in the licensed portions of the spectrum demonstrating that allocated spectrum is under-utilized. Thus, what was basically thought of, as an apparent scarcity of spectrum is actually the result of the under-utilization caused by existing spectrum allocation policies [1]. Hence, the need for a novel spectrum allocation policy has been identified.

The basic objective of the new spectrum allocation policy is the promotion of secondary utilization of unused portions of the spectrum in the form of *spectrum*

pooling, wherein, unlicensed users rent licensed portions of the spectrum from a common pool of spectral resources from different owners [3]. This improves the utilization of the spectral resources while potentially generating additional revenue to the licensed users. However, the implementation of a spectrum pooling system raises many technological, economic and political questions, that need to be answered for the successful coexistence of the legacy[1]and rental systems. Efficient pooling of the radio spectrum is achieved by using a *cognitive radio* [4], which is a multi-band, spectrally agile radio that employs flexible communication techniques and detects the presence of primary user transmissions over different spectral ranges to avoid interference to the licensed users.

Orthogonal Frequency Division Multiplexing (OFDM) is a promising candidate in the physical layer design of any multi-band, spectrally agile radio, since it can achieve high data rate communications by collectively utilizing a number of orthogonally spaced frequency bands which are modulated by many slower data streams [3]. Moreover, this division of the available spectrum into a number of orthogonal subcarriers makes the transmission system robust to multipath channel fading [5]. Furthermore, it is possible to turn off the subcarriers in the vicinity of the primary user transmissions, and thus the spectral white spaces can be filled up efficiently [6].

The focus of this research is OFDM transmission over contiguous and non-contiguous frequency bands in Dynamic Spectrum Access (DSA) channels. The basic idea is to improve the system performance of an OFDM-based cognitive radio by solving an important problem that makes the coexistence of the legacy

[1]In this thesis, the terms *legacy systems* and *primary systems* are used to refer to the licensed owners of the RF spectrum whereas the terms *rental systems* and *secondary systems* are used to refer to the users that utilize the idle licensed portions of the spectrum.

and the rental systems a practical solution to the existing under-utilization of the radio spectrum.

1.2 Research Objective

The problem in question is the interference suffered by the legacy system that is present in the vicinity of the bands used by the rental system. This is a result of using OFDM, which is the de-facto multiplexing scheme in most of the spectrum pooling based cognitive radio systems [3]. As OFDM uses *sinc*-type pulses in representing the symbols transmitted over all the subcarriers during one time instant, the large sidelobes that occur can potentially interfere with the signal transmissions of the neighboring legacy systems or with the transmissions of other rental users. Thus, the fundamental objective of this thesis is to develop algorithms which reduce the interference caused by the secondary user while not significantly affecting the system performance of the rental user.

Sidelobe suppression in OFDM-based cognitive radio systems is a relatively unexplored area of research. Even though OFDM-based transceiver systems are the research focus of many groups at different universities all over the world, only a few sidelobe suppression techniques are available in the technical literature [7–11]. Existing algorithms achieve a significant amount of interference suppression at the cost of transmitting a considerable amount of side information to the receiver or at the cost of an increased number of computations at the transmitter. Therefore, it is important to develop algorithms that find a solution while maintaining the system complexity at a reasonable minimum and/or with no side information. An attempt has been made to provide a solution to the problem of interference caused by the rental user which meets the requirements outlined above. In other words,

algorithms which do not sacrifice system performance and which do not need any side information to be transmitted have been proposed.

Before moving on to the thesis contributions, a brief introduction to the current state-of-the-art is provided in the following section.

1.3 Current State-of-the-art

The concepts of spectrum pooling and cognitive radio were first introduced in [4]. This paper outlines the basic factors that need to be considered in determining the pooling strategy and in designing the radio etiquette. [12] provides an understanding and mathematical analysis of the design principles behind the architecture of a software defined radio. Other physical design issues such as the adaptive nature of the transmitter both in selecting the frequency range over wideband frequencies, the different power levels, and the signal processing involved at the receiver, which are important aspects in the design of a cognitive radio, have been discussed at length in [13]. Further insight into the notion of spectrum pooling is provided by another seminal paper by Dr. Timo A. Weiss and Dr. Friedrich K. Jondral in [3]. Some of the issues pertaining to spectrum pooling that are detailed in this paper include: detecting a spectrum, collecting and broadcasting the spectrum access measurements, and mutual interference caused by a rental system to a legacy system and vice-versa. Mutual interference in OFDM-based spectrum pooling systems is discussed in greater detail in [7]. This paper also discusses simple techniques to counter the effects of mutual interference caused by the sidelobes of an OFDM symbol in a spectrum pooling scenario.

OFDM-based transceiver systems have been proposed to be the viable solution for building a spectrum pooling system in [3]. The fundamental advantages of

using OFDM in a spectrum pooling based cognitive radio are: the flexibility in filling up the spectral gaps left behind by the licensed users in their idle periods, turning off the subcarriers in the frequency bands used by the licensed users by transmitting zeros [6] and the inherent frequency sub-banding [14]. Moreover, in an OFDM-based transceiver, a high data-rate stream is converted to many parallel slower data substreams. This allows for support to a high data-rate system as well as being robust to channel impairments.

An important challenge in the physical layer design of an OFDM-based cognitive radio is the interference caused by an unlicensed system to the licensed systems or other unlicensed systems in the neighboring frequency bands. However, only a few research groups are focusing on sidelobe suppression resulting from the OFDM-based rental systems. Some of the algorithms proposed are: sidelobe suppression by insertion of cancellation carriers [9], wherein a few subcarriers on either side of the OFDM signal spectrum carry weights calculated using optimization and help in sidelobe suppression, by subcarrier weighting [10], wherein the symbols carried by the subcarriers are weighted using optimization techniques, and through multiple choice sequences (MCS) [11], wherein the symbol sequence carried by the subcarriers is mapped to another low sidelobe symbol sequence calculated by a variety of techniques. However, when the number of subcarriers is large and when the modulation scheme used is high, using optimization schemes to calculated the weights of the cancellation carriers and the symbol sequence is a complex procedure. Also, in the case of using MCS, there is a large amount of side information to be transmitted to the receiver for proper demodulation, and hence a reduction in the system throughput.

1.4 Thesis Contributions

This thesis presents the following two novel algorithms for sidelobe suppression in OFDM-based cognitive radios in a DSA environment:

- A cancellation carrier (CC) based algebraic technique which calculates the interference power level that needs to be minimized at the desired frequency location. Then, a cancellation carrier is inserted whose amplitude is scaled in such a way that, it has a sidelobe at the desired frequency location that nulls the calculated interference. Applying this procedure on both sides of the OFDM spectrum, a suppression of around 15 dB is achieved when two cancellation carriers are used on either side of the QPSK-OFDM spectrum in a 64 subcarrier system.

- A constellation expansion based technique, in which each symbol of a particular constellation space is associated with symbols from a higher order constellation diagram. This procedure exploits the fact that different symbol sequences have different sidelobe levels and hence, by associating more than one point from the higher order constellation space to every symbol in the original constellation diagram, a particular sequence is selected iteratively whose sidelobe power levels are the lowest. Using this procedure, a suppression of around 10 dB is achieved in a QPSK-OFDM system with 64 subcarriers.

The proposed cancellation carrier technique, does not rely on complex optimization procedures and the weights carried by the CCs are calculated algebraically. Hence, the complexity of the algorithm does not increase with the number of subcarriers in the system or with the increase in the order of the modulation

scheme. Similarly, the constellation expansion based approach, does not require any side information to be transmitted to the receiver, but achieves significant amount of suppression in the sidelobe power levels.

1.5 Thesis Organization

This thesis is organized as follows: Chapter 2 provides a brief introduction to the concept of a cognitive radio and an overview of some of the basic principles of an OFDM-based transceiver.

Chapter 3 gives an introduction to the mutual interference caused in a scenario with the coexistence of the the licensed and unlicensed users. Interference caused by the rental system to a legacy system, which is the focus of this thesis is explained in detail. Also discussed is the impact of the interference suppression on the coexistence of the licensed and unlicensed systems. The existing techniques for reducing this impact are outlined and their shortcomings are listed.

In Chapter 4, the proposed techniques for sidelobe suppression are explained in detail and the simulation results obtained are presented. A detailed discussion about the obtained results is also provided.

Finally, in Chapter 5, several conclusions are drawn and directions for future research are presented.

Chapter 2

OFDM-based Cognitive Radio

This chapter provides an introduction to the concepts of spectrum pooling-based cognitive radio and orthogonal frequency division multiplexing (OFDM). The efficiency of an OFDM-based cognitive radio in helping the secondary utilization of the RF spectrum and its system performance evaluation is also discussed.

2.1 A Spectrum Pooling-based Cognitive Radio for Flexible Wireless Communications

The demand for more spectral resources to support the growing number of sophisticated applications of wireless radio devices and the number of wireless mobile phone users is ever increasing. In the process of finding a solution for supplying the limited spectral resources to the almost unlimited demand for more spectrum, the Federal Communications Commission (FCC)'s spectral efficiency working group made a key observation about the traditional spectrum allocation policies. That is, allotting fixed portions of the spectrum to the licensed users causes a potential waste of the spectral resources since the licensed spectrum is

heavily underutilized over time and frequency [1]. Therefore a whole new policy needs to be formulated wherein secondary utilization of the licensed spectrum can be encouraged while ensuring that the system performance of the licensed user is not compromised. This new policy is called "spectrum pooling".

The notion of "spectrum pooling", first introduced in [4] is a mechanism for pooling the spectral resources from different spectral owners and renting these spectral resources to unlicensed users during idle periods. However, such a lease of licensed spectral resources to rental users while providing additional revenue to the licensed users brings forth many technological, jurisdicial, economic and political questions concerning the regulatory aspects of spectrum pooling. The technical challenges that need to be solved to make spectrum pooling practical have been the research focus of numerous groups at universities all over the world.

Flexible pooling of the spectral resources is made possible by cognitive radio, an extension of software-defined radio, which autonomously and dynamically determines the appropriate transceiver parameters based on its interaction with the environment, to enable secondary utilization of the spectrum [15]. Such a radio that is cognitive towards the changing operating parameters has to employ agile physical layer transmission techniques in order to respect the rights of the incumbent licensed users, and reconfigurable hardware that makes the adaptation to changing environmental conditions feasible [16]. Moreover, a formal radio etiquette needs to be formulated, which is a framework to moderate the use of the RF spectrum for guaranteeing the rights of the licensed users as well as for the flexible coordination between the unlicensed users. Some of the basic issues that need to be considered with respect to the radio etiquette as outlined in [4] are:

- ***The renting process***: a customary sequence of events during which the

renter and the offerer communicate through a standardized signalling protocol regarding access to the unutilized portion of the licensed spectrum,

- ***Assured polite backoff to the authorized legacy radios***: the process in which the legacy system can reclaim the spectral resources, and the rental system discontinues its use of the spectrum
- ***Precedence and priority criteria***: a formalized algorithm to guarantee the availability of the spectrum to the users
- ***An order-wire network***: a knowledge exchange language for the sharing of control information regarding the changing environment parameters.

An important issue in the renting process is the detection of the idle spectral ranges by the rental user. This can be achieved by employing dynamic spectral access (DSA) techniques, wherein the main objective is to reliably detect the idle spectral ranges, while keeping the false alarm probability of identifying an idle spectral range as occupied, to be low. A high detection probability is directly related to the system throughput of the rental system, as this assures protection of the rights of the licensed users to the spectrum they own, as well as a guarantee to the rental system that idle spectral ranges are not left undetected.

A complete description and mathematical analysis of the topological properties of the software-defined radio (SDR) architecture is provided in [12]. A detailed mathematical perspective of the principles that define the design of a SDR help in characterizing the interfaces among hardware, middleware and higher level software components that are needed for cost-effective plug-and-play services.

2.2 An Overview of Orthogonal Frequency Division Multiplexing (OFDM)

The mobile radio channel is contaminated with multipath fading, *i.e.,* the transmitted signal is reflected by various terrain sources and multiple reflected copies of the signal arrive at the receiver at different times. These reflected, delayed versions of the signal interfere with the direct line-of-sight (LOS) wave and cause intersymbol interference (ISI) which results in significant degradation of the system performance. Even though adaptive equalizers can be employed at the receiver to mitigate the effects of ISI when the transmission data rate is of the order of kilobits per second, such a setup would become extremely complex and expensive when the transmission bit rate is of the order of several megabits per second. To overcome the effects of such a multipath fading environment, a parallel data transmission scheme needs to be used which reduces the influence of multipath fading and makes the use of complex equalizers unnecessary.

2.2.1 Introduction

In a classical parallel data transmission system that uses frequency division multiplexing (FDM), the carriers are spaced apart in frequency in such a way that the signal carried by each carrier can be filtered and demodulated. This is done by using guard carriers to avoid the spectral overlap of the channels, and hence, there is a huge waste of the RF spectrum, resulting in inefficient use of the spectrum. This situation is depicted in Figure 2.1 (a) [5]. However, it is possible to allow the overlap of the individual subcarriers without leaving spectral guard bands, and still be able to avoid the adjacent subcarrier interference. This is the case, when the individual subcarriers' center frequencies are orthogonal. In other words, if

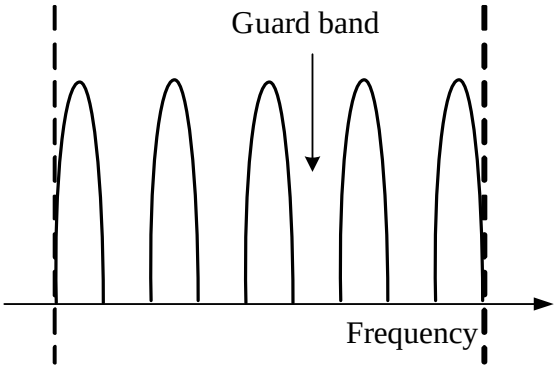

(a) Conventional FDM-based multicarrier technique

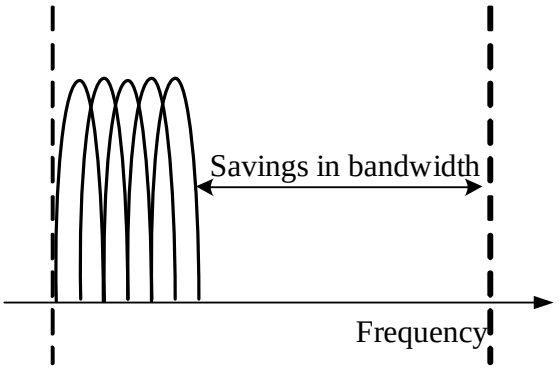

(b) Orthogonal FDM-based multicarrier technique

Figure 2.1. An illustration of the conventional and orthogonal FDM techniques

the symbol duration in time domain is T, then if the carrier spacing between the individual subcarriers is a multiple of $1/T$, there is no crosstalk between the overlapping subcarriers. This is depicted in Figure 2.1 (b). From this figure, the resulting bandwidth savings can also be observed.

Applying inverse discrete fourier transform (IDFT) and discrete fourier transform (DFT) for modulation and demodulation processes respectively, as proposed in the seminal paper [17] by Weinstein and Ebert, the OFDM signal spectrum of a $N = 8$ subcarrier system is as shown in Figure 2.2. It can be observed from this figure that, at the center frequency of each subcarrier, there is no in-

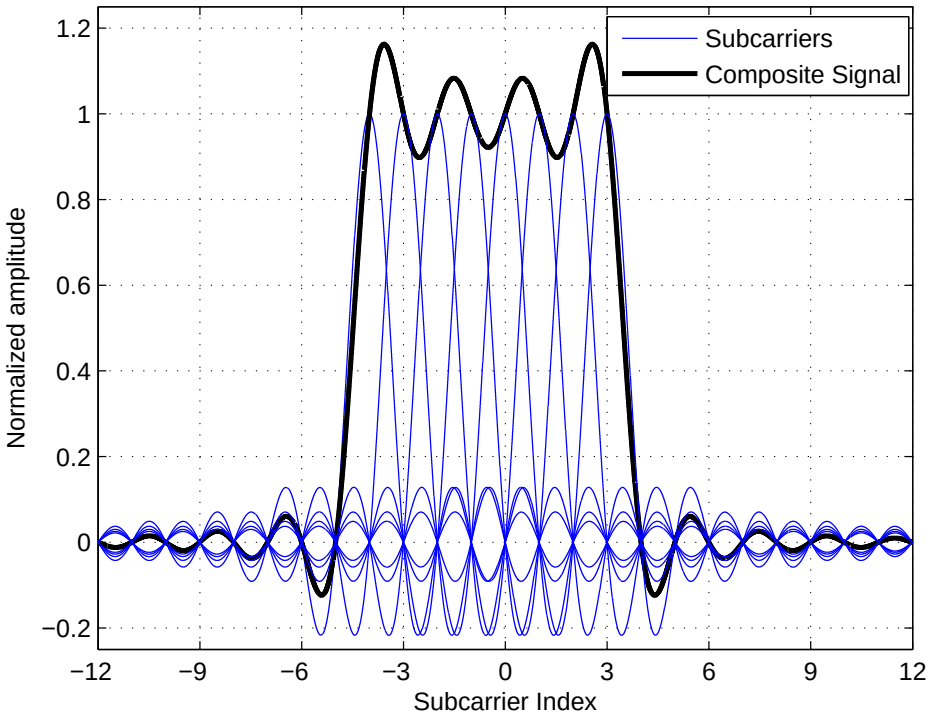

Figure 2.2. OFDM signal spectrum of a N=8 subcarrier OFDM transceiver using DFT

terference due to the other subcarriers, and hence the transmitted signal can be recovered at the receiver by translating each center frequency to DC and applying an integrate-and-dump operation. Moreover, with the advancements in the field of very-large-scale integration (VLSI) technology, a complete digital implementation of the OFDM transceiver can be built using special purpose hardware which perform fast fourier transform (FFT), an efficient implementation of DFT.

The earliest development of a parallel data transmission system can be traced back to 1958 [18] followed by the work by Saltzberg [19], Weinstein and Ebert [17] and Hirosaki [20]. The number of applications involving OFDM has steadily increased in the form of technologies like, wideband data communications over mobile radio FM channels, high-bit-rate digital subscriber lines (HDSL; 1.6$Mbps$),

asymmetric digital subscriber lines (ADSL; $6Mbps$), very-high-speed digital subscriber lines (VDSL; $100Mbps$), digital audio broadcasting (DAB), highdefinition television (HDTV) terrestrial broadcasting, IEEE 802.11a/g and IEEE 802.16a [5].

The following subsections in this section give a brief overview of the different basic principles concerning OFDM.

2.2.2 A general schematic of an OFDM-based cognitive radio transceiver

In this subsection, the process of generating an OFDM signal and its characteristics are explained with the help of the general schematic of an OFDM-based transceiver [16] shown in fig. 2.3.

Let $\mathbf{d}=(d_1, d_2, ..., d_n)$ be a data stream modulated to $\mathbf{x}=(x_1, x_2, ..., x_n)$ by an M-ary Phase Shift Keying (MPSK) or an M-ary quadrature amplitude modulation (M-QAM) modulator. The modulated data stream is then split into N slower data streams using a serial-to-parallel (S/P) converter. Each of these streams is transmitted on one of the N orthogonal subcarriers and then summed up to give a composite OFDM signal. In a DSA environment, it is difficult to obtain a contiguous block of spectrum. So, the subcarriers that are located in the bands used for licensed user accesses are turned off. This decision is made by employing dynamic spectrum sensing and channel access techniques. This information regarding the subcarriers that are being used for signal transmission is also sent to the receiver. OFDM-based transceivers that are capable of deactivating the subcarriers based on the spectrum sensing methods are referred to as *non-contiguous* OFDM (NC-OFDM)-based transceivers [2]. If, $X_{k,m}$, $m = 0, 1, ..., N-1$ represents the complex modulated symbol over subcarrier, m at the k-th instant of

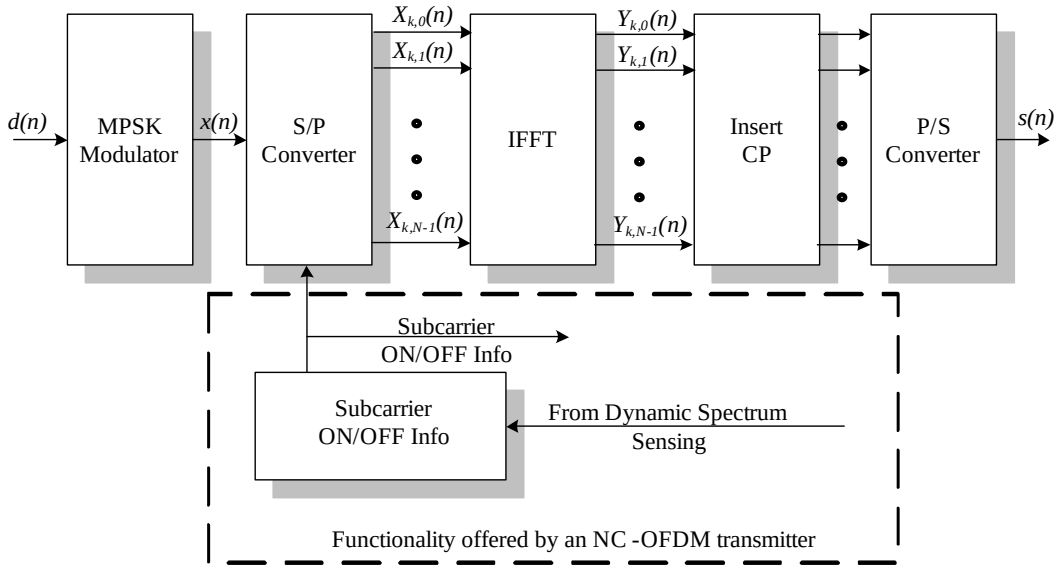

(a) A general OFDM-based transmitter

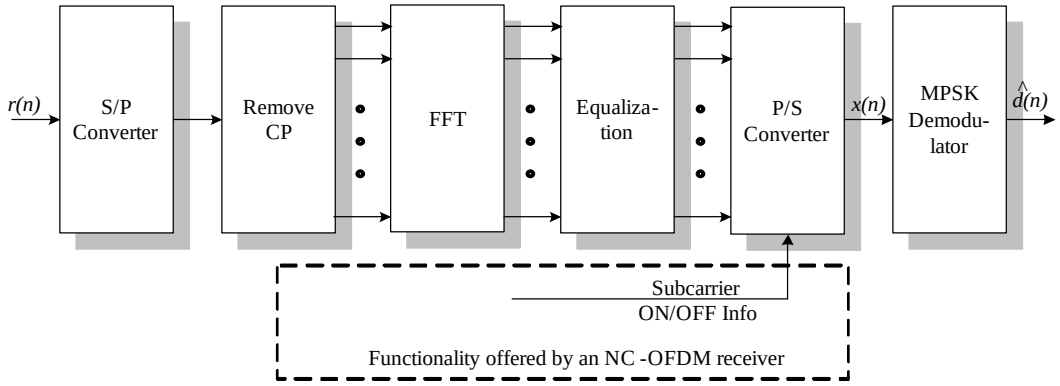

(b) A general OFDM-based receiver

Figure 2.3. A general schematic of an OFDM-based cognitive radio transceiver

time, then one baseband OFDM symbol, multiplexing N subcarriers is given by,

$$s_k(t) = \frac{1}{N} \sum_{m=0}^{N-1} X_{k,m} e^{j2\pi f_m t} \qquad 0 < t < NT \tag{2.1}$$

where T is the symbol duration and

$$f_m = \frac{m}{NT} \qquad m = 0, 1, ..., N-1$$

are the equally spaced orthogonal subcarrier frequencies, f_m. In order to implement equation Eq. (2.1) requires in-phase and quadrature-phase matched filter banks. An alternate modulation practice is to perform T-spaced sampling of the above OFDM symbol over both the in-phase and the quadrature-phase components, which yields,

$$s_k(nT) = \frac{1}{N} \sum_{m=0}^{N-1} X_{k,m} e^{j2\pi f_m nT} \qquad 0 \leqslant n \leqslant N-1. \tag{2.2}$$

This operation is nothing more than performing an inverse discrete fourier transform (IDFT) [21] over $x_{k,m}$, which was one of the key properties proposed by Weinstein and Ebert in [17]. In the block diagram of Figure 2.3, this is performed by the inverse fast fourier transform (IFFT) block, which is an efficient way of performing IDFT.

Going back to the example of a $N = 8$ subcarrier system considered in Figure 2.2, the time domain representation will typically appear as shown in Figure 2.4 and the composite OFDM symbol as shown in Figure 2.5. An important problem in transmitting the signal generated in the above equation is that the orthogonality between the subcarriers is lost when transmitting through a dispersive channel. In addition to the intercarrier interference (ICI) caused by this loss of orthogonality, multiple delayed copies of the transmitted signal result in intersymbol interference (ISI) between successive symbols. An intelligent way of dealing with this problem is to attach a cyclic prefix to the OFDM symbol, a concept introduced in [22]. However, this cyclic extension of the OFDM symbol helps in combating the effects of dispersive channel as long as the channel delay is smaller than the cyclic prefix. By the property of the cyclic convolution, discarding the cyclic prefix before taking the FFT at the receiver eliminates the ISI. Nevertheless, the use of a cyclic prefix

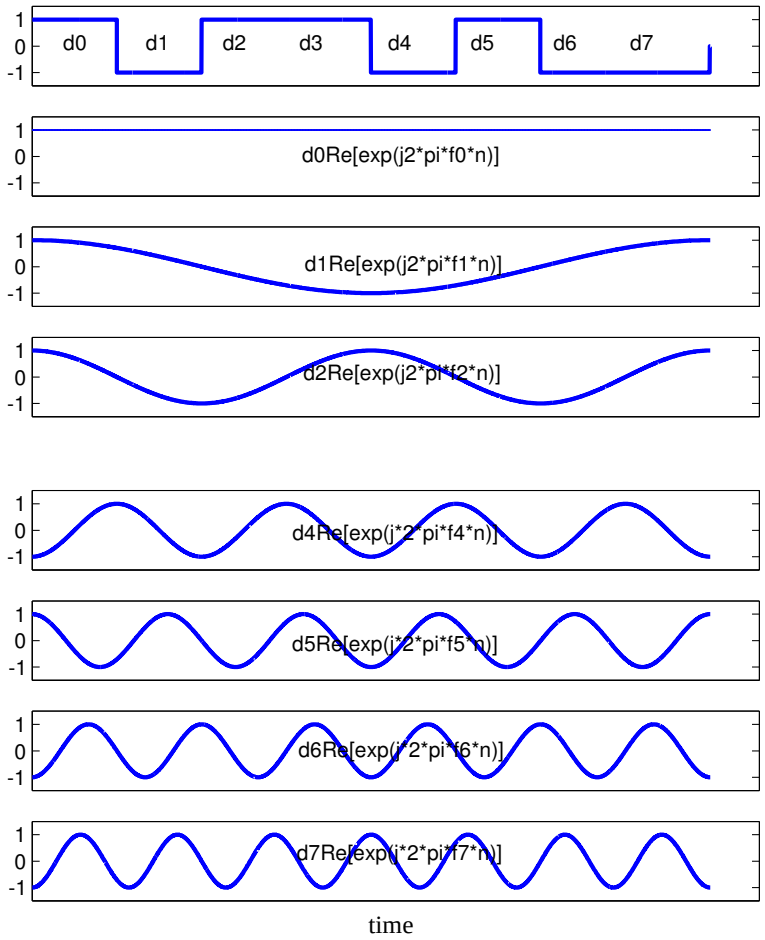

Figure 2.4. An illustration showing the time domain waveforms of a N=8 subcarrier OFDM transceiver system that are summed to create parallel data signals

requires more transmit energy, which can be reduced by making the symbol period longer than the cyclic prefix. Similarly, by employing simple one-tap N parallel equalizers, ICI is mitigated. After adding a cyclic prefix to the OFDM symbol, it is passed through a parallel-to-serial (P/S) converter, then the signal is upsampled and passed through a digital to analog (D/A) converter for converting it into an analog signal, followed by lowpass filtering. Then, the signal is translated to the desired bandpass frequency and amplified by a power amplifier.

At the receiver, the signal is translated to baseband, lowpass filtered and con-

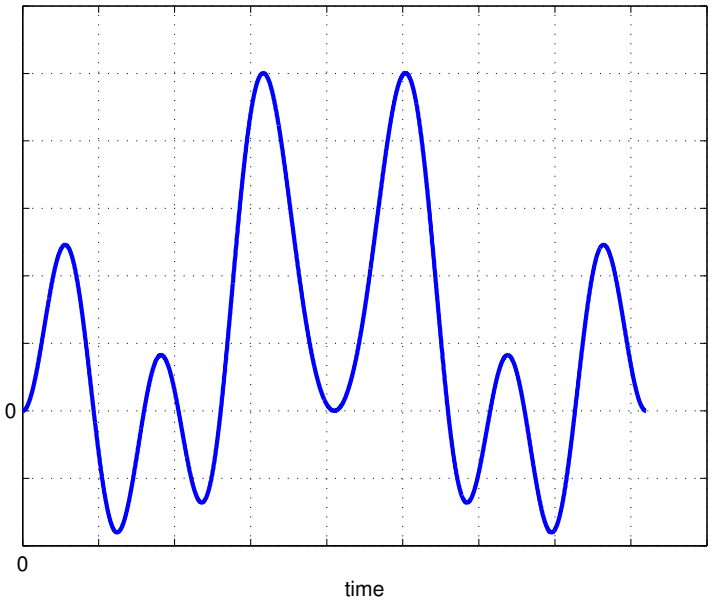

Figure 2.5. An illustration showing the time domain composite OFDM symbol of the N=8 subcarrier OFDM transceiver system

verted to a digital signal by passing through an analog-to-digital (A/D) converter. By passing through a S/P converter, this digital data stream is converted to $N+l$ parallel streams, where l is the number of symbols added as cyclic prefix. These l symbols are discarded next, before performing the DFT operation,

$$\hat{X}_{k,m} = \sum_{n=0}^{N-1} r_{n,m} e^{j2\pi \frac{mn}{N}} \qquad n = 0, 1, ..., N-1 \tag{2.3}$$

The remaining N parallel streams are converted to a serial stream using a P/S converter and then demodulated to obtain an estimate of the transmitted data stream.

2.2.3 Channel model

In the presence of a dispersive channel and additive white gaussian noise (AWGN), the k-th received OFDM symbol is,

$$Y_k = H_k X_k + n_k \qquad k = 0, 1, ..., N-1 \tag{2.4}$$

where n_k is the FFT of the sampled noise terms $n_t(nT)$, $n = 0, 1, ..., N-1$. The received noise which is usually white, is also white after performing the FFT. Also, $H_k = FFT(h_k)$ is the frequency response of the channel, h_k is the impulse response of the dispersive channel. The multipath channel whose impulse response is h_k has the form [23],

$$h(\tau) = \sum_{m=0}^{M} a_m \delta(\tau - \tau_m) \tag{2.5}$$

where M is the number of multipath components, a_m is a zero-mean complex gaussian independent random variable, and τ_m is the delay associated with the m-th path. Also, the power delay profile assumed is exponential [24], *i.e.,*

$$E[h(\tau)h^*(\tau)] = Ce^{-\tau/\tau_{rms}} \qquad 0 < \tau < \tau_{max} \tag{2.6}$$

where τ_{rms} is the RMS delay spread, τ_{max} is the maximum delay spread and C is a normalization constant which makes the total multipath power equal to unity.

It can be noted from Eq. (2.4) that simple one-tap frequency domain equalization can be employed to remove the effects of flat fading. That is, the received signal over path m is multiplying with $1/a_m$. However, this process also enhances the noise by a factor of $1/a_m^2$. In order to perform the equalization mentioned above, channel estimation is necessary. [25] proposes the use of pilot-symbol as-

sisted modulation (PSAM) which involves sparse insertion of known pilot symbols in a stream of data symbols. The attenuation suffered by the data symbols is estimated by measuring the attenuation suffered by the pilot symbols using time-correlation properties of the fading channel. The concept of PSAM also allows the use of frequency correlation properties of the channel. Also, in a properly designed OFDM system, the subcarrier spacing is small compared to the coherence bandwidth of the channel, and therefore, there is significant amount of correlation between the attenuation suffered by adjacent subcarriers. Similarly, as the symbol duration is small compared to the coherence time of the channel, the time correlation between the channel attenuations of the consecutive symbols is high. Thus, both the time correlation as well as the frequency correlation can be exploited by a channel estimator. The form the channel estimator is determined by the choice of the pilot pattern.

In order to better combat the effects the channel dispersion, it has been proposed that the operating system parameters, such as the choice of the modulation scheme and/or the power level of each subcarrier, can be modified to each subchannel. By applying adaptive modulation, or bit loading, which is the process of assigning a particular scheme to a subcarrier based on the knowledge of the environment, the system can be optimized given an error constraint or the bit error rate can be reduced given a throughput limit. Similarly, optimum power allocation to each subcarrier can be employed in tandem with bit allocation to meet either of the two requirements mentioned above. Further information regarding the various bit and power allocation schemes can be found at [26].

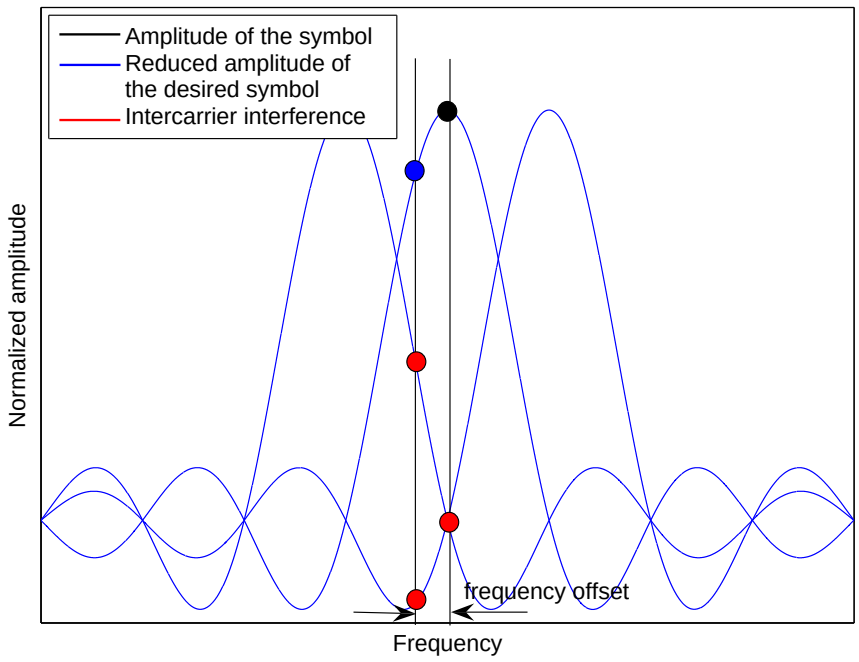

Figure 2.6. An illustration showing the effect of ICI to the desired OFDM symbol due to frequency offset

2.2.4 Synchronization in OFDM-based transceiver systems

Fig. 2.6 illustrates the most important effect of a frequency offset between the transmitter and the receiver of an OFDM-based cognitive radio. The effect is two-fold. The amplitude of the desired symbol is reduced in addition to the introduction of interference from the adjacent carriers. Frequency offsets are a result of the oscillator impairments and sample clock differences at the front-end of the receiver. The translation of the received signal to baseband involves the use of oscillators which need to be synchronized with those at the transmitter. The following two equations [25] illustrate the degradation, D (in dB) as a function of frequency offset normalized to the intercarrier spacing $(1/NT)$, ε, in AWGN and

fading channels respectively,

$$D \approx \frac{10}{3\ln 10}(\pi\varepsilon)^2\frac{E_s}{N_0} \tag{2.7}$$

$$D \leq 10\log\left[\frac{1+0.5947\frac{E_s}{N_0}\sin^2\pi\varepsilon}{sinc^2\varepsilon}\right]^2 \tag{2.8}$$

In addition, unwanted phase modulation and symbol timing errors due to sample clock offsets further degrade the SNR.

An effective way of achieving carrier synchronization and channel estimation is to send a known preamble before each OFDM frame to the receiver. In the Digital Video Broadcasting (DVB-T) system and the wireless LAN systems like IEEE 802.11a and HIPERLAN/2, certain subcarriers are used as continuous pilots. These subcarriers are boosted by a certain factor and carry known data, which is used for frequency synchronization and estimation of Doppler bandwidth by Weiner filtering [27]. The Doppler bandwidth can be estimated from the continuous pilots (after frequency-shift correction) by standard power spectral density estimation methods. Wireless LAN systems require a fast frequency synchronization at the beginning of every burst. As a result, a special OFDM symbol, has been defined at the beginning of every burst, in which 12 subcarriers are modulated to serve as a frequency reference [27]. For time synchronization, the EU147 Digital Audio Broadcasting (DAB) system uses a null symbol which can be detected by a traditional analog envelope detector [27]. In the DAB system, the first OFDM symbol after the null symbol serves as reference. In the wireless LAN systems, IEEE 802.11a and HIPERLAN/2, a reference OFDM symbol of twice the normal symbol duration is used for timing synchronization.

2.2.5 Peak-to-average power ratio

Peak-to-average power ratio (PAPR) is an important physical layer design problem in OFDM-based transceivers. PAPR is the principal focus of various OFDM-based research groups at many universities. Significant research has also been done at The University of Kansas [2].

As the OFDM signal is the sum of a large number of independent, identically distributed components, its amplitude has an approximately Gaussian distribution, by central limit theorem [25]. So, very high peaks appear in the transmitted signal. This property is measured by the signal's peak-to-average power ratio which is defined as [2],

$$PAPR(s(t)) = \frac{\max\limits_{0\leq t\leq T} |s(t)|^2}{E\{|s(t)|^2\}} \tag{2.9}$$

where

$$s(t) = \frac{1}{N}\sum_{m=0}^{N-1} x_k e^{j2\pi kt/T} \tag{2.10}$$

is the complex envelope of the baseband signal consisting of N contiguous subcarriers over a time interval [0, T], x_k is the symbol on the k-th subcarrier and T is the OFDM symbol time duration. Also, $E\{.\}$ in Eq. (2.9) denotes the expectation operator. To be able to transmit and receive these high peaks requires expensive high-precision A/D and D/A converters and power amplifiers with large back-off. A simple clipping of the OFDM signal will not efficiently solve the problem, as it causes spectral spillage and large degradation in BER.

As an illustration, consider a $N = 16$ subcarrier BPSK-OFDM transceiver system. When the input symbols are all ones, the normalized power of the OFDM symbol in time domain is shown in Figure 2.7 (a). From this figure, the mean

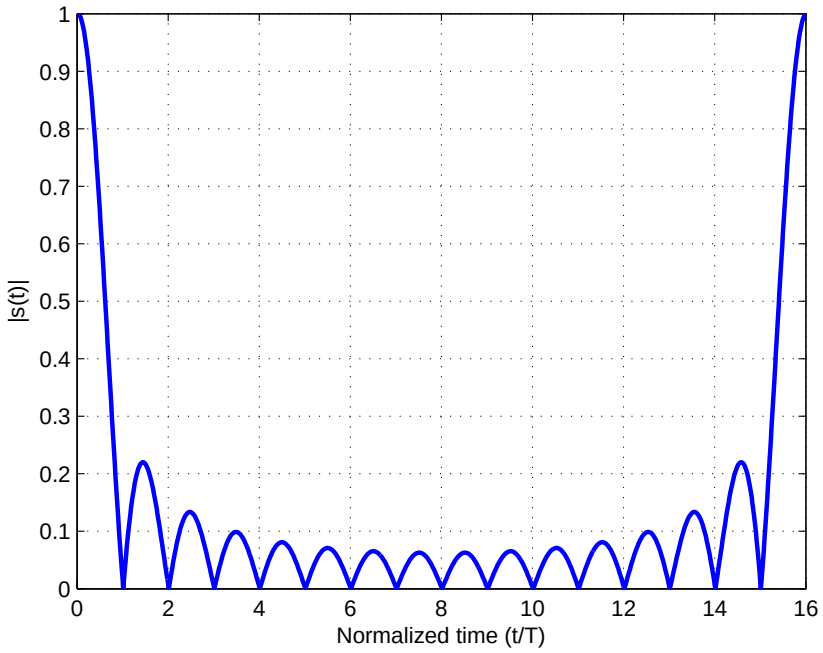

(a) Time-domain OFDM transmit signal when the subcarriers carry an all ones

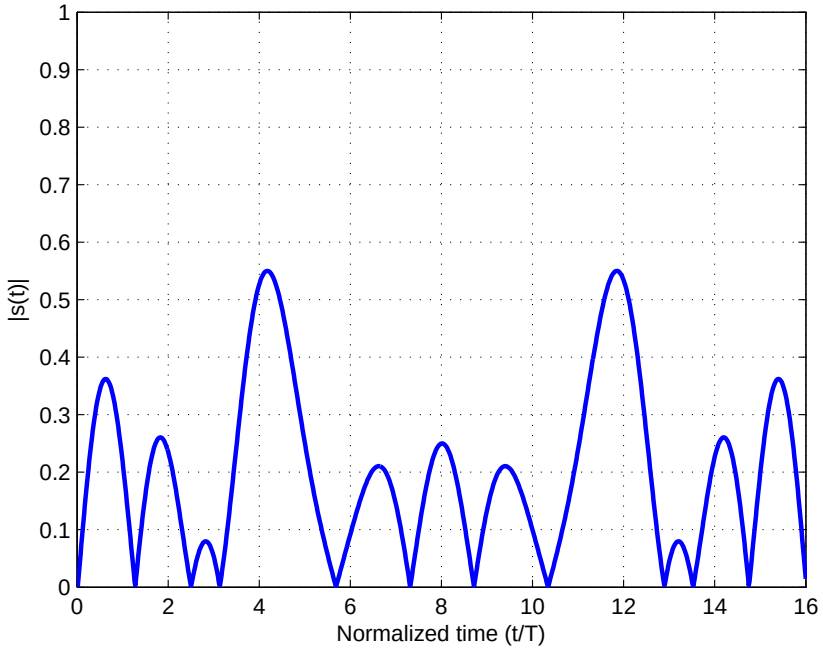

(b) Time-domain OFDM transmit signal when the subcarriers carry a random sequence

Figure 2.7. An illustration showing the time domain waveforms of a N=16 subcarrier BPSK-OFDM transceiver system

power of the signal can be calculated to be 0.0625 and the peak power is unity. The PAPR of the signal is 16. Now, consider an input random sequence, [1 1 1 -1 1 1 -1 -1 1 1 -1 -1 1 -1 -1 -1]. The normalized power of the OFDM symbol in time domain is shown in Figure 2.7 (b). The mean power of the signal remains 0.0625 as the total power of the signal remains constant. However, the peak power is 0.3025. Thus, the PAPR is equal to 4.8407. This figure, illustrates that the random sequence that is being transmitted has an effect on the PAPR of the signal. Moreover, it has been suggested that the sequences with the maximum correlation yield a very high PAPR value [28]. Some of the algorithms proposed in the literature aim at reducing the correlation of the sequence to reduce the PAPR. Furthermore, the PAPR of a system is directly related to the number of subcarriers in the system. Greater the number of subcarriers, larger is the PAPR.

A detailed description of the PAPR problem and a taxonomy of the existing techniques can be found in [2].

The next chapter deals with another important issue: out-of-band radiation resulting from the use of OFDM. The focus of this research is to develop algorithms to mitigate the effects of this problem.

Chapter 3

Out-of-band Interference Problem in OFDM

The concept of spectrum pooling was proposed as an answer to the efforts of the FCC to promote the secondary utilization of the RF spectrum. Also, OFDM has proved to be the ideal technique for use in cognitive radios to make the implementation of spectrum pooling feasible. Even though OFDM-based cognitive radios have proven to be ideal in efficiently filling up the spectral white spaces left unused by the licensed systems, there is an important challenge that needs to be solved for the coexistence of the legacy and rental systems in the RF spectrum. The sidelobes resulting from the use of OFDM for representing the symbols of the low data rate streams, are a source of interference to the legacy systems or other rental systems that might be present in the vicinity of the spectrum used by the unlicensed system. Conversely, in the presence of a non-orthogonal rental system, the system performance of the secondary system might suffer from interference. This chapter focuses on the problem of out-of-band interference in OFDM-based transceivers resulting from the rental system.

3.1 Interference to the Legacy System

With respect to the interference caused by the unlicensed user to the licensed user, the important issue that needs to be taken into consideration when designing an OFDM-based overlay system is that its impact on the legacy system should be very small. Thus, the basic aim of any algorithm for sidelobe suppression is to reduce the sidelobe power levels while causing little or no effect to the other secondary system parameters. Before moving on to a summary of the existing algorithms for sidelobe suppression, a brief mathematical representation of the interference to the legacy system and two simple techniques for mitigating the its effects are provided in this section.

Assuming the transmit signal, *s(t)* on each subcarrier of the OFDM-transceiver system is a rectangular non-return-to-zero (NRZ) signal, the power spectral density of *s(t)* is represented in the form [29]

$$\Phi_{ss}(f) = A^2 T \left(\frac{\sin \pi f T}{\pi f T} \right)^2 \tag{3.1}$$

where A denotes the signal amplitude and T is the symbol duration which consists of the sum of symbol duration, T_S and guard interval, T_G. The assumption that the transmit signal *s(t)* on each subcarrier is a rectangular NRZ signal is valid since it matches the wireless LAN standards [30], [31]. Now assuming that, the legacy system is located in the vicinity of the rental system, the mean relative interference, $P_{Interference}(n)$, to a legacy system subband is defined as [7]:

$$P_{Interference}(n) = \frac{1}{P_{Total}} \int_{n}^{n+1} \Phi_{ss}(f) df \tag{3.2}$$

where P_{Total} is the total transmit power emitted on one subcarrier and n represents

the distance between the considered subcarrier and the legacy system in multiples of Δf.

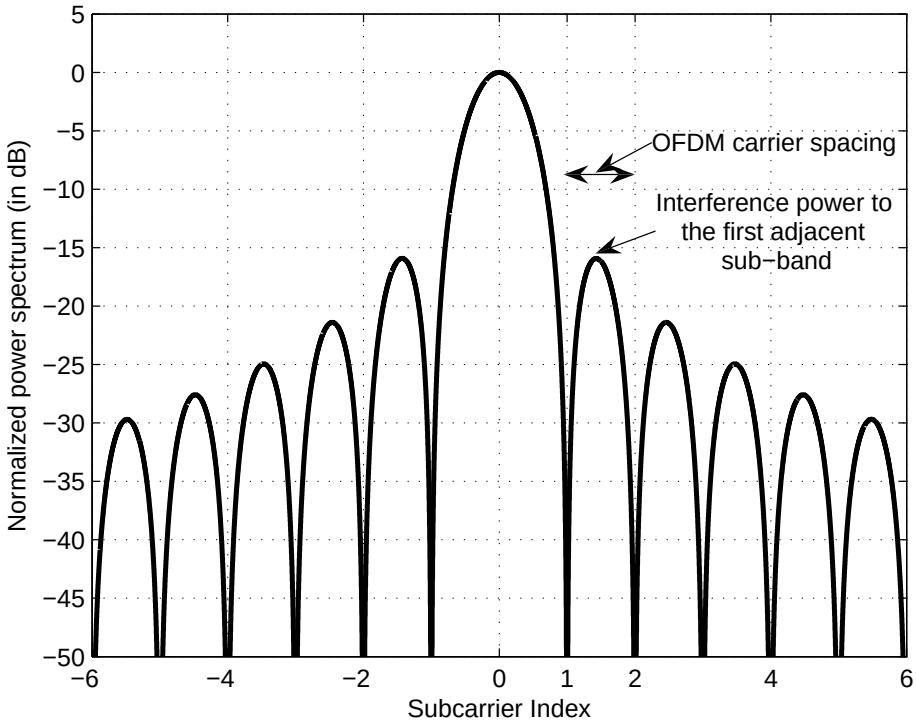

Figure 3.1. An illustration of the interference due to one OFDM-modulated carrier

As an illustration, Figure 3.1 shows the power spectral density of an OFDM modulated carrier. This figure shows the subcarrer spacing and the interference power due to the first sidelobe in the first adjacent band. It is observed that as the distance between the location of the subcarrier of the rental system and the considered subband increases, the interference caused by it reduces monotonically, which is a characteristic of the *sinc* pulse. However, it should also be noted that in a practical scenario consisting of N subcarriers, the actual value of the interference caused in a particular legacy system subband is a function of the random symbols carried by the *sinc* pulses and N.

The idea of interference calculation for the case of one subcarrier can be extended to a system with N subcarriers. Let $s_n(x),\ n = 1, 2, 3, ..., N$, be the subcarrier of index n represented in the frequency domain. Then,

$$s_n(x) = a_n \frac{\sin(\pi(x - x_n))}{\pi(x - x_n)}, \qquad n = 1, 2, ..., N. \tag{3.3}$$

In the above equation, $\mathbf{a} = [a_1\ a_2\ ....\ a_N]^T$ is a data symbol array, x is a normalized frequency given by:

$$x = (f - f_0)T$$

where f denotes the frequency and f_0 is the center frequency. Also, x_n is the normalized center frequency of the nth subcarrier. Again, the signal in the time domain at the transmitter is assumed to be in a rectangular NRZ form. Now, the OFDM symbol in the frequency domain over the N subcarriers is:

$$S(x) = \sum_{n=1}^{N} s_n(x). \tag{3.4}$$

The power spectral density of the above signal is given by:

$$\Phi_{ss}(f) = |S(x)|^2 = \left| \sum_{n=1}^{N} a_n \frac{\sin(\pi(x - x_n))}{\pi(x - x_n)} \right|^2 \tag{3.5}$$

As an example, a BPSK-OFDM system with $N = 16$ subcarriers is considered. When the vector $\mathbf{a} = [1\ 1\ 1\ 1\ 1\ 1\ 1\ 1\ 1\ 1\ 1\ 1\ 1\ 1\ 1\ 1]^T$, Figure 3.2 shows the normalized OFDM power spectrum. As shown in this figure, the portion of the signal indicated in dashed lines represents the potential interference causing sidelobes resulting from summing up the sinc pulses that carry the symbols from the data vector. Also, the Figure 3.2 is for the case where the data vector consists of ones,

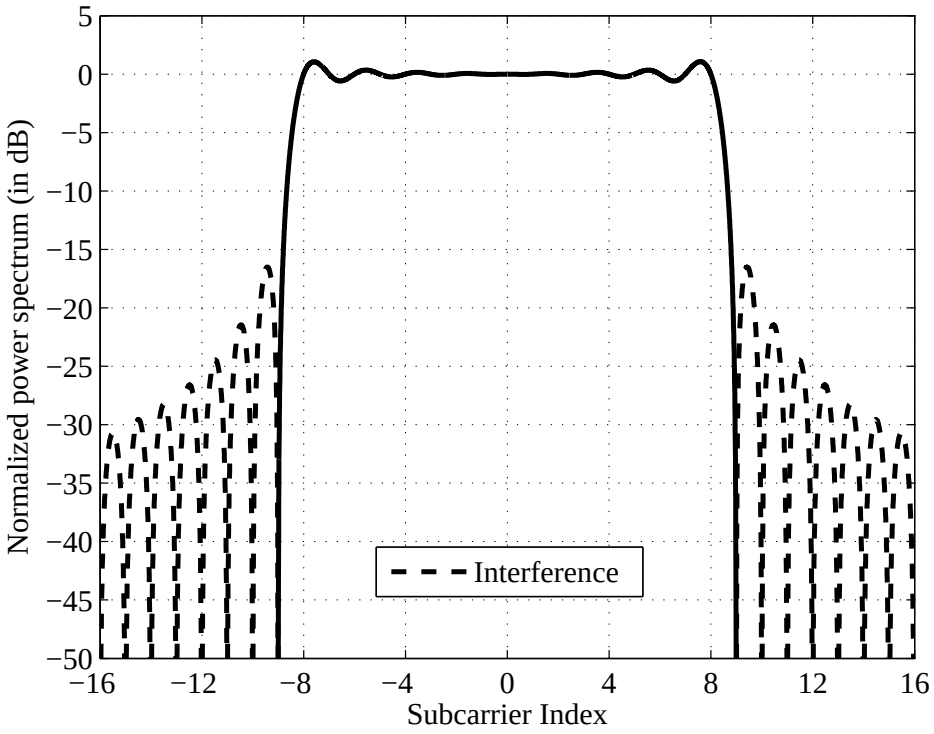

Figure 3.2. An illustration of the interference in a BPSK-OFDM system with N=16 subcarriers

and hence, depending on the random distribution of the symbols, the sidelobe power levels decay at different rates.

3.1.1 Windowing: A simple countermeasure to the interference from rental system

One of the simplest and the earliest solutions offered to counter the effects of OOB interference is windowing the OFDM transmit signal in the time domain

[7,8]. A raised cosine window defined by:

$$w(t) = \begin{cases} \frac{1}{2} + \frac{1}{2}\cos\left(\pi + \frac{\pi t}{\beta T}\right), & \text{for } 0 \leq t < \beta T \\ 1, & \text{for } \beta T \leq t < T \\ \frac{1}{2} + \frac{1}{2}\cos\left(\frac{\pi(t-T)}{\beta T}\right), & \text{for } T \leq t < (1+\beta)T \end{cases} \tag{3.6}$$

is a commonly used window type where β is defined as the rolloff factor. Applying the transmit filter, $w(t)$, the OFDM signal in time-domain is as shown in Figure 3.3. It can be noted from this figure that the postfix needs to be longer than βT to maintain the orthogonality within the OFDM signal. That is, the application of windowing to reduce the OOB radiation of the OFDM signal has the adverse effect of expanding the temporal symbol duration by $(1+\beta)$, resulting in a lowered system throughput for the unlicensed user.

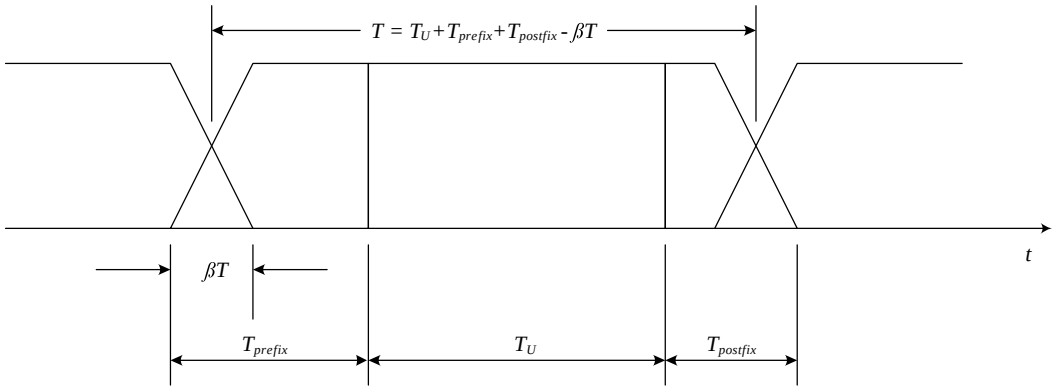

Figure 3.3. Structure of the temporal OFDM signal using a raised cosine window

The impact of the rolloff factor of the window on the sidelobe power levels of the OFDM symbol is depicted in Figure 3.4. It can be observed from this figure that for smaller values of β, the suppression achieved in the sidelobe power levels of the first adjacent band is very small. As the distance between the location of

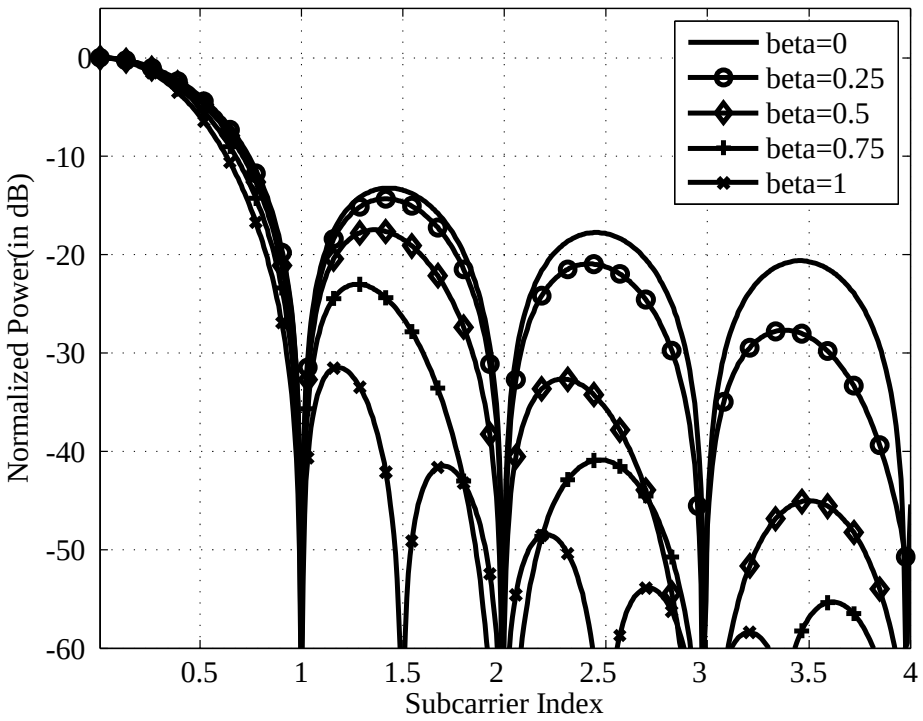

Figure 3.4. Impact of rolloff factor on the PSD of the rental system signal.

the subcarrier of the rental system and the considered subband increases, the suppression achieved also increases. Also, for very large values of β, the suppression achieved is considerably high even in the case of the first adjacent band. However, the symbol duration in time is also increased, which reduces the system throughput. Thus, windowing can be applied as an additional means to suppress the high sidelobes, but more powerful techniques need to be developed.

3.1.2 Insertion of guard bands: Another simple technique for interference suppression

Fig. 3.5 shows another technique for mitigating the effects of the sidelobes from the secondary user's OFDM symbols on the system performance of the legacy

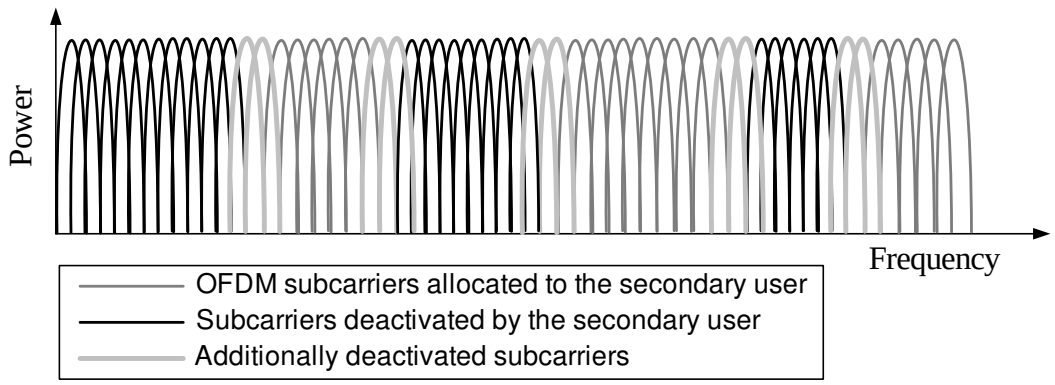

Figure 3.5. An illustration of the guard band technique for sidelobe suppression

system. The idea is to deactivate additional subcarriers in the vicinity of the licensed user that are allotted to the unlicensed user in addition to those that are deactivated due to licensed user accesses [7]. In Figure 3.5, the subcarriers indicated in black are the bands which are deactivated by the secondary user due to the licensed user accesses. The subcarriers shown in dark gray indicate the region in the spectrum which are being used by the secondary user. The subcarriers indicated in light gray are the ones which are allocated to the secondary user, but are left unused to reduce the amount of the sidelobe power leaking into the spectral region that is being used by the licensed user. With this technique, there is a waste of the already scarce spectral resources. Moreover, the reduction achieved is not significant enough, as shown in Figure 3.6.

In this figure, a BPSK-OFDM system with $N = 64$ subcarriers is considered. The simulations were performed over 20,000 symbols. From Figure 3.6 (a), it can be observed that, by inserting two guard carriers on each side of the spectrum, the achievable average reduction of the maximum interference causing sidelobe is only $2.8dB$ and by inserting eight guard carriers, the reduction achieved is around $4.6dB$. A significant reduction of around 10 dB can be achieved, by giving

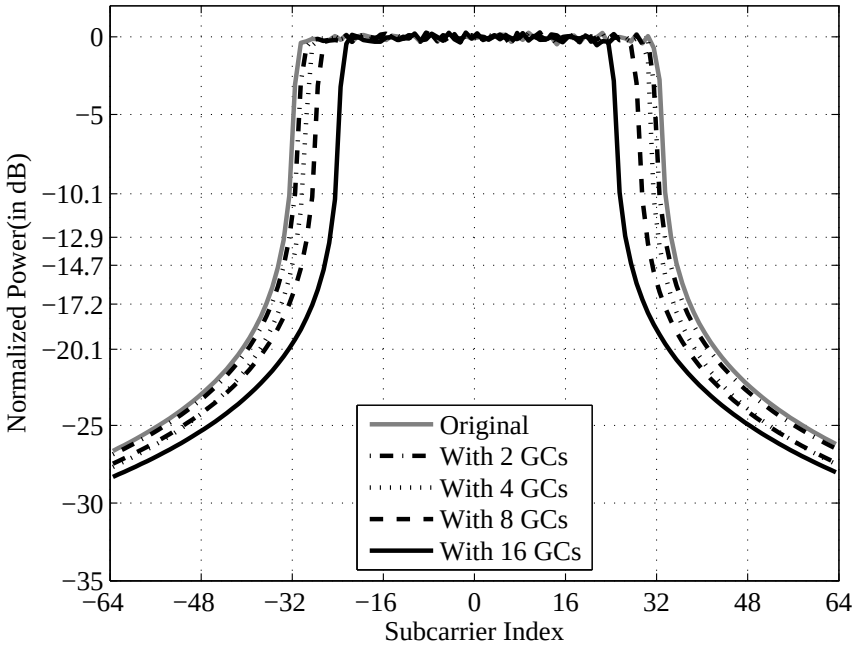

(a) Normalized power spectrum plot

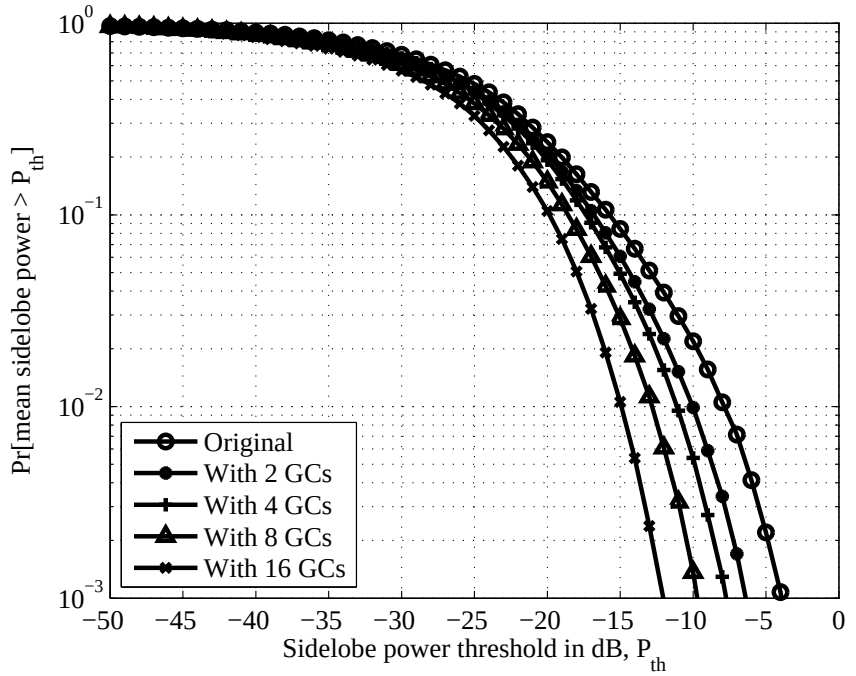

(b) Complementary cumulative distribution function (CCDF) plot

Figure 3.6. Interference suppression in a BPSK-OFDM system with N=64 subcarriers by inserting guard bands

up 25% of the allocated bandwidth *i.e.,* by using 16 subcarriers out of 64 for inserting guard bands. The complementary cumulative distribution function of Figure 3.6 (b) also illustrates the same point. On average, 99.9% of the sidelobe power is below $-3.8dB$ in the original case, whereas by inserting two guard carrier on each side of the OFDM spectrum, the value is $-8.7dB$ and by inserting eight guard carriers, the value is around $-15dB$.

3.2 A brief summary of the existing Sidelobe Suppression Techniques

The area of sidelobe suppression is a relatively unexplored area of research concerning OFDM-based cognitive radios. Significant work has been done by groups at the DoCoMo Communications Laboratories, Munich, Germany and at the German Aerospace Center (DLR), Inst. of Communications and Navigation, Wessling, Germany, respectively.

A technique of inserting cancellation carriers has been proposed in [9]. In this technique, few cancellation carriers are inserted on either side of the OFDM spectrum with precomputed weights. The weights are computed by selecting an optimization region, which is the portion of the neighboring RF spectrum over which the sidelobes need to be suppressed, and finding an optimal solution. The optimization is formulated as a linear least squares problem, solved using a singular value decomposition approach. The proposed technique achieves a suppression of $14.6dB$ in a $N = 56$ subcarrier QPSK-OFDM system, with $M = 8$ cancellation carriers. Also, using this approach, there is a BER degradation of $1.25dB$ and a PAPR augmentation of $0.27dB$.

In another technique proposed in [10], the symbols carried by all the subcar-

riers are optimally weighted. Again, the weights are precomputed using complex optimization techniques. Using this technique, in order to achieve a suppression of $15.8dB$, in an $N = 12$ subcarrier QPSK-OFDM system, there is an associated BER degradation of 0.0231 at $\gamma_b = 14dB$. As stated earlier, these two techniques suffer from increased computational complexity when the number of active subcarriers is high in number and/or when the modulation scheme is of higher order.

Another technique proposed in [11] exploits the fact that different symbol sequences have different sidelobe power levels, and hence proposes transmitting the symbol sequence with the lowest sidelobe power levels instead of the generated symbol sequence. Furthermore, this paper also provides the different means of generating random symbol sequences, like symbol constellation mapping, interleaving, and random phase updating. Numerical results from this paper show that, to achieve a sidelobe suppression of $14.5dB$, there is a throughput reduction of 29%, as side information needs to be transmitted to the receiver, for correctly decoding the transmitted symbol sequence. Higher suppression of interference is also achieved by applying the proposed techniques, but the amount of side information that needs to be transmitted also increases greatly.

In the paper, [32], a technique for reducing the PAPR of the OFDM signal is proposed. Using this technique, in addition to achieving a PAPR reduction of around $2.5dB$ at 0.1% PAPR for $K = 3$ interleavers using 5-APSK, a sidelobe suppression of around $10dB$ is observed. However, the authors note this effect only a secondary advantage of using their technique, and PAPR reduction was the intended result.

All the above techniques and the ones presented in the following chapter are

aimed at suppressing the interference from the rental system to the legacy system. For a brief overview of the techniques aimed at mitigating the effects of interference from the legacy system to the rental system, refer [33].

In the following chapter, a description of the proposed techniques as well as a comparison with the existing ones is provided.

Chapter 4

Proposed Techniques for Sidelobe Suppression

In this chapter, a detailed description of the two proposed algorithms is provided. In the first algorithm, a fixed number of subcarriers are used to cancel out the interference that might result from the transmitted OFDM symbol. In the second algorithm, the symbols that are being transmitted are mapped to symbols from a higher constellation and the sequence with the lowest sidelobe power level is transmitted.

4.1 Proposed Sidelobe Suppression using Cancellation Carriers

In this section, a novel low complexity algebraic algorithm for suppressing the sidelobes of the OFDM symbol which result in the out-of-band (OOB) interference is discussed. The proposed technique is evaluated within the framework of an OFDM as well as an NC-OFDM transceiver. Simulations results are shown which

prove the effectiveness of the proposed technique.

4.1.1 Schematic of an OFDM transceiver employing cancellation carriers for sidelobe suppression

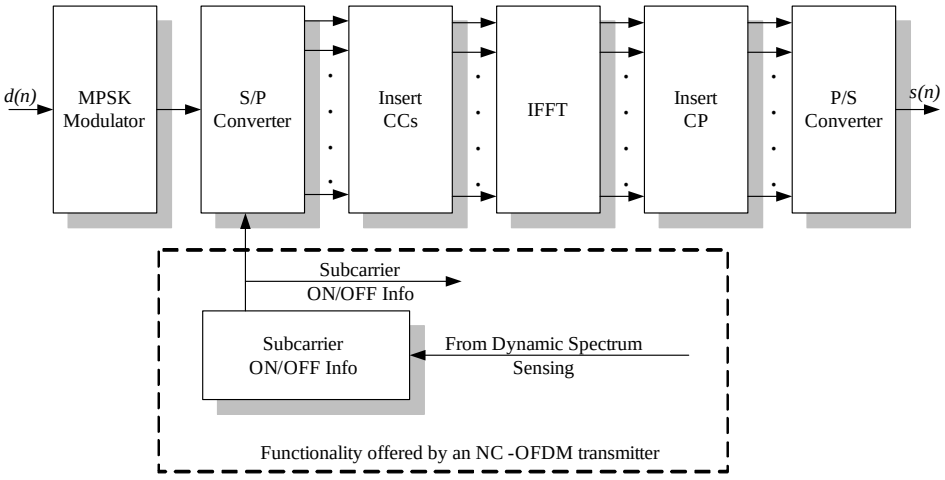

(a) An OFDM-based transmitter employing the CC technique

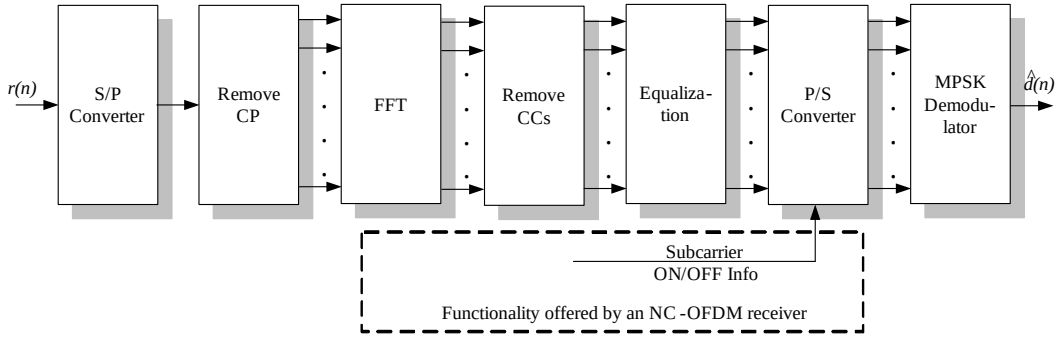

(b) An OFDM-based receiver employing the CC technique

Figure 4.1. Schematic of an OFDM-based cognitive radio transceiver employing the proposed sidelobe suppression technique.

A general schematic of the OFDM transceiver employing the proposed sidelobe suppression technique is shown in Fig. 4.1. A high speed data stream, *x(n)* is modulated using M-ary phase shift keying (MPSK). The modulated data stream is split into N slower data streams using a serial-to-parallel (S/P) converter. In the presence of primary user transmissions, which are detected using DSA and

channel estimation techniques, the secondary OFDM user turns off the subcarriers in their vicinity resulting in a non-contiguous transmission. Of the remaining active subcarriers, a small fraction is used for cancelling out the OOB interference arising from the OFDM symbols used in the secondary signal transmission. The IFFT is then applied to these modulated signals. A cyclic prefix (CP) whose length is greater than the delay spread of the channel is inserted to mitigate the effects of the intersymbol interference (ISI). Following the parallel-to-serial (S/P) conversion, the baseband OFDM signal is passed through the transmitter's RF chain, to amplify the signal and upconvert it to the desired frequency.

At the receiver, the reverse operations are performed, namely, mixing the bandpass signal to downconvert it to a baseband signal, then applying S/P conversion, discarding the cyclic prefix and applying FFT to transform the time domain signal to frequency domain. As the symbols over the cancellation carriers do not carry any information, they are discarded. After performing channel equalization and P/S conversion, the symbol stream is demodulated to recover the original high-speed input.

4.1.2 Proposed sidelobe suppression technique

Several sidelobe suppression techniques have been proposed in the literature. As discussed in the previous chapter, the straightforward techniques include inserting null guard carriers on either side of the OFDM spectrum and transmit windowing [7]. However, these techniques have the inherent disadvantage that, either a portion of the allocated spectrum is left unused or the symbol duration is increased in time domain, which leads to intersymbol interference (ISI). Also, the suppression achieved by employing these techniques is not significant enough

to compensate for the loss of the system performance. A technique based on inserting a few cancellation subcarriers with optimized weights was proposed in [9]. The proposed technique uses a low computational complexity algorithm to determine the amplitude and phase of the cancellation subcarriers (CCs) and hence complex optimization procedures are avoided to achieve a sub-optimal solution. The proposed technique explained in the following paragraphs achieves a mean sidelobe suppression as low as what is achievable using the optimization technique proposed in [9], but avoids complex optimization procedures and instead, uses an algebraic technique to find the weights of the CCs.

Let the number of subcarriers in an OFDM system be N+M. Each of the subcarriers carries an MPSK symbol, d_n, $n = -N/2.....N/2-1$. Modulating these N MPSK symbols whose temporal pulse shape is rectangular to different subcarrier frequencies, results in a sinc-shaped frequency response with large sidelobes. Thus, the spectrum of each subcarrier is given by:

$$s_n(x) = d_n.sinc(x) \tag{4.1}$$

where $n = -N/2.....N/2-1$ and $x\epsilon R$ represents the frequency-shifted to the center frequency, ω_0 and normalized to the subcarrier bandwidth $1/T_0$. The spectrum of the transmitted signal is the superposition of the spectra of the individual subcarriers. Therefore,

$$S(x) = \sum_{n=-N/2}^{N/2-1} s_n(x). \tag{4.2}$$

The remaining M subcarrier (with $\frac{M}{2}$ on each side) center frequencies are cancellation subcarriers, where cancellation carrier are inserted. The subcarriers inserted at these locations carry no information and are instrumental in cancelling

the out-of-band (OOB) interference only. The basic principle of the *sinc*-pulses that is being exploited here is, as the *sinc*-pulses decay monotonically with frequency in the OOB region, the total OOB radiation power at any location in the OOB region, is nothing but a sum of the power contained in each *sinc*-pulse at that location. That is, if the interference at the $k = (-N/2 - M/2 - 1)$th center frequency is I_k, then:

$$I_k = \sum_{n=-N/2}^{N/2-1} d_n.sinc(k). \tag{4.3}$$

The cancellation subcarrier at $-N/2 - 1$ location is inserted in such a way that the interference at the kth location is minimized. Proceeding in a similar manner, the CC at the $(-N/2 - M/2)$th location is inserted to minimize the interference at the $(-N/2 - M)$th location.

As an illustration of the proposed technique, consider the OFDM symbol shown in Fig.4.2 where $N + M = 16$, $M = 2$ and the symbol sequence on the active subcarriers is [1 1 1 1 1 1 1 1 1 1 1 1 1 1]. In this case, if I_k^l is the interference at the kth location, the scale of the CC, C_j^l is in such a way that, the interference is minimized. Also, depending on the random modulation symbols, the sidelobes will decrease monotonically and so, the first cancellation carrier will minimize the interference at the desired location and will cause the interference at other locations to decrease as well. However, in order for the sidelobes to be further suppressed, successive cancellation carriers are needed. Nevertheless, cancellation carriers as low as two in number will cause a potential reduction in the sidelobe power levels. The complexity of the proposed algorithm can be reduced further, by taking into consideration the fact that the subcarriers that are closer to the desired location where interference needs to be suppressed contribute more than the subcarriers that are farther. Therefore, the simulation results show that even

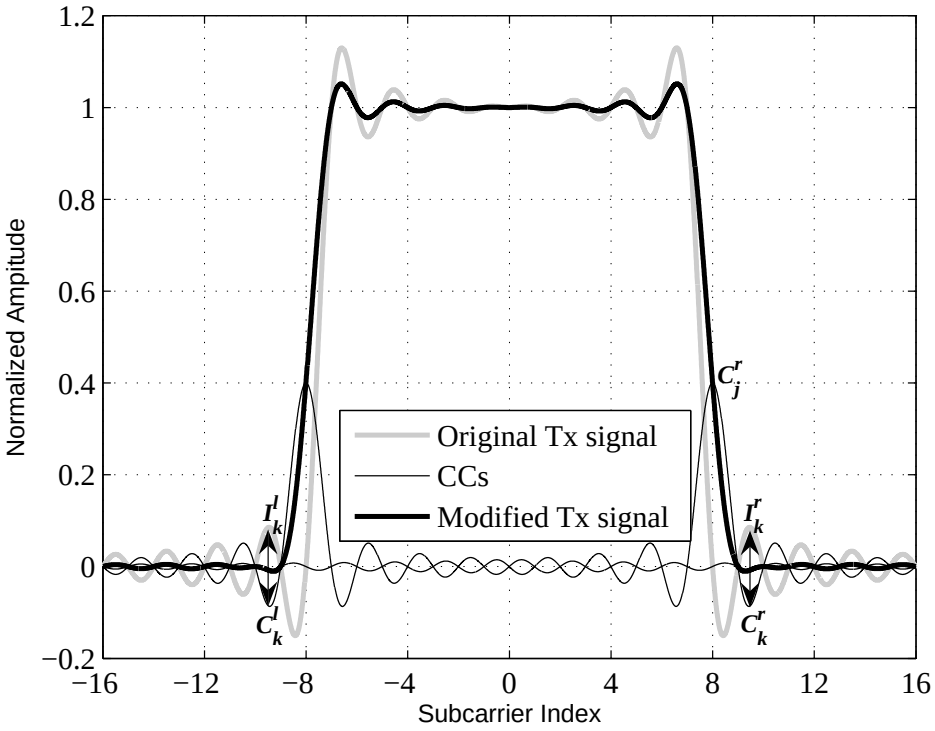

Figure 4.2. An illustration of the sidelobe suppression using the proposed technique.

estimates of the interference cause sufficient reduction in the interference power levels.

4.1.3 Simulation Results

4.1.3.1 Simulation Parameters

The proposed is evaluated for 50,000 randomly generated BPSK-OFDM and QPSK-OFDM symbols over contiguous and non-contiguous set of active subcarriers. The number of subcarriers in the considered spectral whitespace is 64, in the contiguous case. The subcarrier bandwidth is kept constant throughout the simulation. In the spectrum sharing scenario, two cases are considered. First,

when the spectral whitespaces are of unequal bandwidth and the spectral gaps between the whitespaces, which are occupied by the primary user, are of constant bandwidth. Second, when the gaps between the spectral whitespaces are of unequal bandwidth.

4.1.3.2 Results

Figures 4.3 and 4.4 show the BPSK-OFDM and QPSK-OFDM for one and two CCs on either side of the spectrum. From the Figures 4.3(a) and 4.3(b), it can be observed that the mean power spectrum reduces by about 2.8 dB for the BPSK-OFDM case when only one null guard carrier (GC) is present and by about 4.9 dB when two guard carriers are present. On the other hand, one CC achieves a reduction of about 10.3 dB and two CCs achieve a reduction of around 14.8 dB. The results for the mean suppression in the case of a QPSK-OFDM system for one and two CCs show similar suppression values. This shows that the CC technique is effective in suppressing the OOB interference. An important point to be noted is that by inserting two CCs, there is an improvement in the interference suppression by about $4.5dB$. However, when inserting the second algorithm, it has been ensured that the sidelobe regrowth over the location, which has been suppressed to zero by the first CC, is kept to a minimum.

The complementary cumulative distribution function (CCDF) plots shown in Figure 4.5 provide further insight into the efficiency of the CCs in suppressing the OFDM sidelobes. From Figure 4.5(a), it can be noted that 0.1% of the OOB interference power of a BPSK-OFDM transmission is reduced by around 10dB. In other words, in the original case, without either GCs or CCs, 99.9% of the OOB power is below 5dB whereas by using two CCs on each side of the spectrum, 99.9%

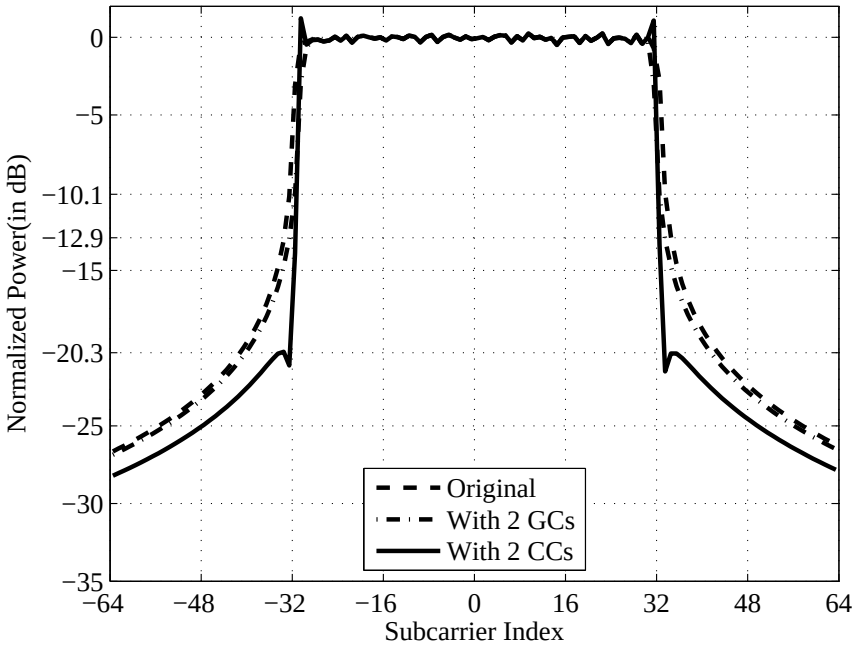

(a) Inserting two CCs

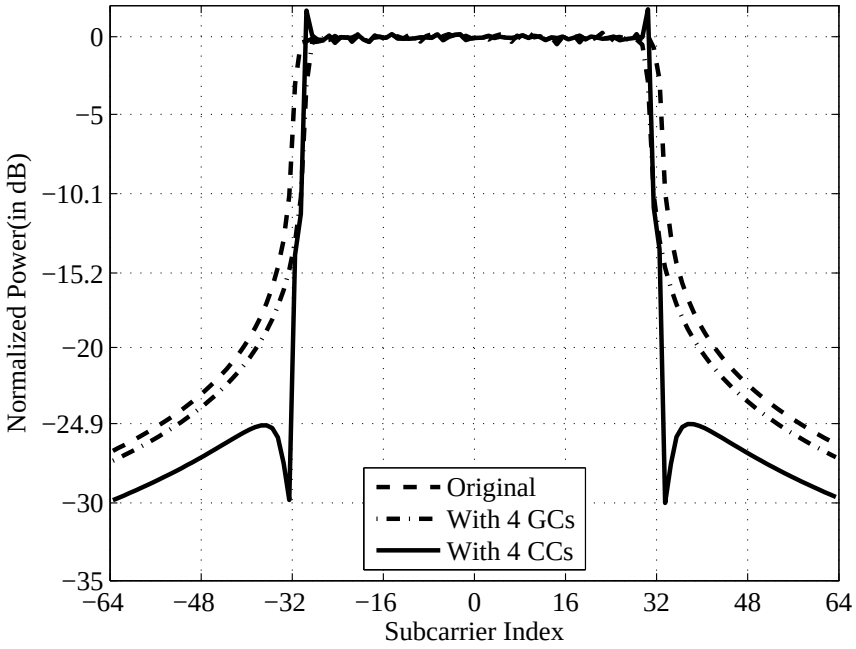

(b) Inserting four CCs

Figure 4.3. Averaged BPSK-OFDM spectrum with and without inserting cancellation carriers(CCs).

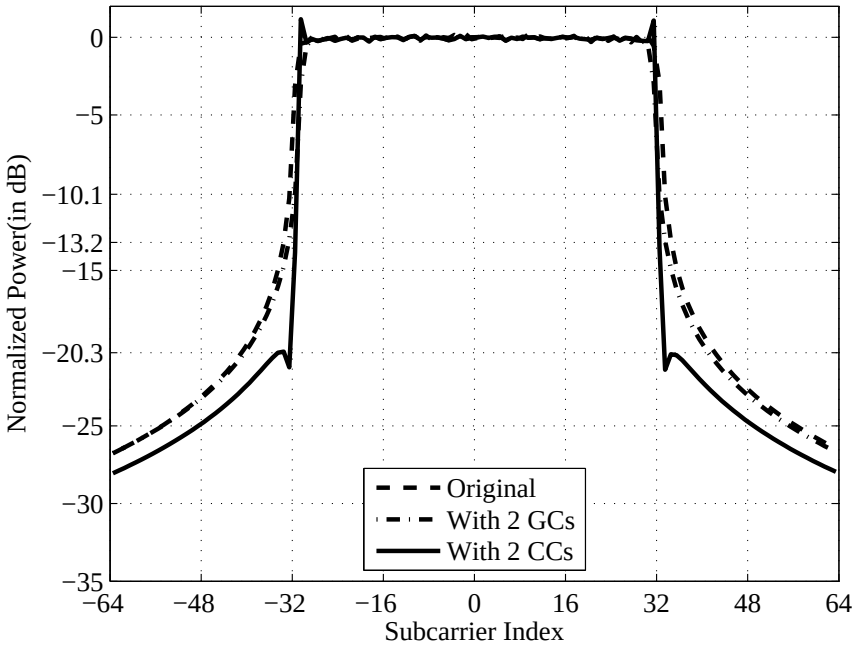

(a) Inserting two CCs

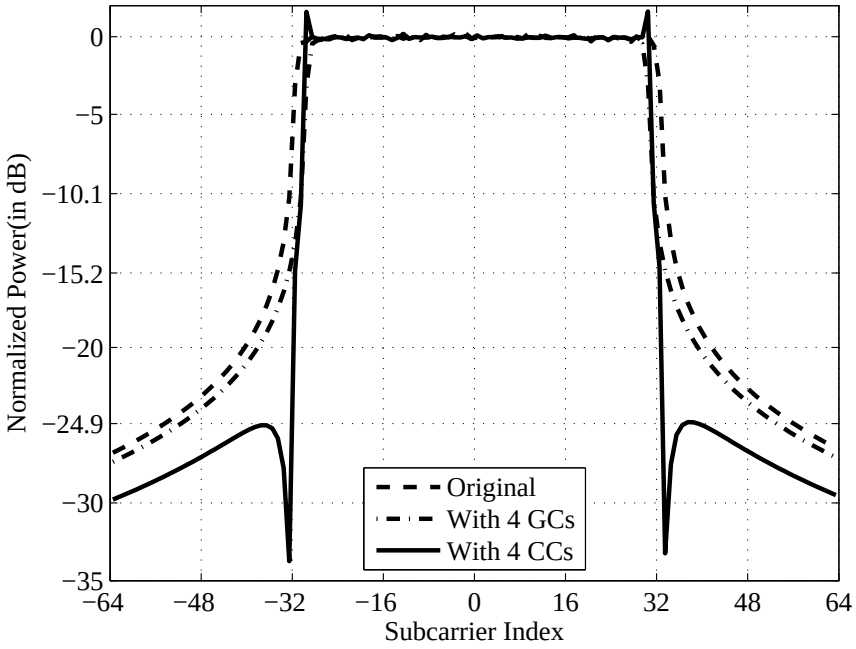

(b) Inserting four CCs

Figure 4.4. Averaged QPSK-OFDM spectrum with and without inserting cancellation carriers(CCs).

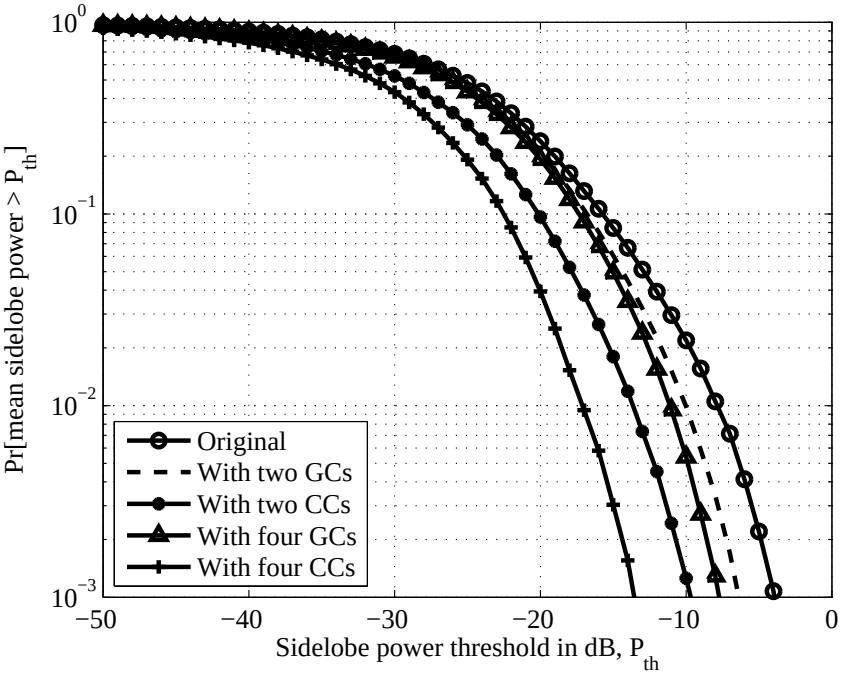

(a) BPSK-modulated OFDM

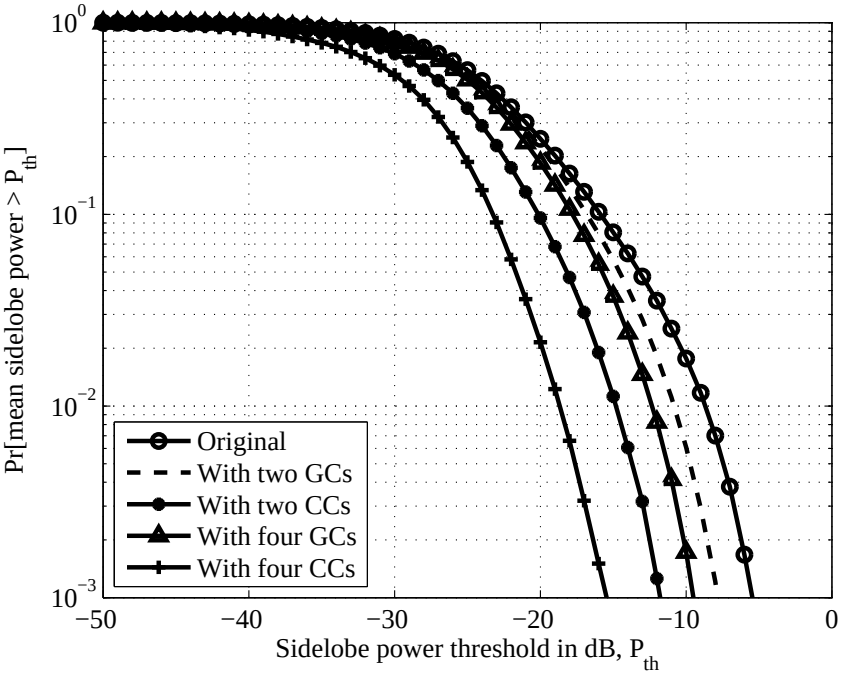

(b) QPSK-modulated OFDM

Figure 4.5. Complementary cumulative distribution function (CCDF) with and without inserting cancellation carriers (CCs).

of the OOB power level is below 15dB. Figure 4.5(b) shows a similar reduction in sidelobe power levels of the QPSK-modulated OFDM system. An interesting point to be noted by observing the normalized power spectrum and the CCDF plots is that by inserting the guard bands, there is a huge loss of spectral resources and a suppression of the sidelobe power that is not commensurate with the loss, whereas in the case of inserting cancellation carriers, with a reasonably small loss in the spectral resources, there is a substantial reduction in the sidelobe power levels.

Figures 4.6 and 4.7 shows the CCDF plot of the sidelobe power levels for BPSK-OFDM and QPSK-OFDM using estimates of the interference level that needs to be suppressed. From Figures 4.6(a) and 4.7(a), it can be observed that, when the number of cancellation carriers is one, even estimates obtained by considering only a fraction of the total subcarriers give sufficiently good performance. However, this statement doesn't hold true when there are two CCs on each side of the spectrum, as shown in Figures 4.6(b) and 4.7(b). The reason behind this occurrence is when there are two CCs on each side of the spectrum, the amplitude and phase of the second CC intended to minimize the interference at a second location have to be selected in such a way that the sidelobe regrowth due to the second CC doesn't affect the interference power level at the location which has already been minimized by the first CC. Also, there is a ceiling of unity on the amplitude level that the CC can have. This is to not violate the transmit power requirements of the considered modulation scheme. Hence, in a few cases, where the interference can be cancelled out only by using a CC of amplitude greater than unity, a unity amplitude CC is used and hence, the interference is made small but not exactly zero.

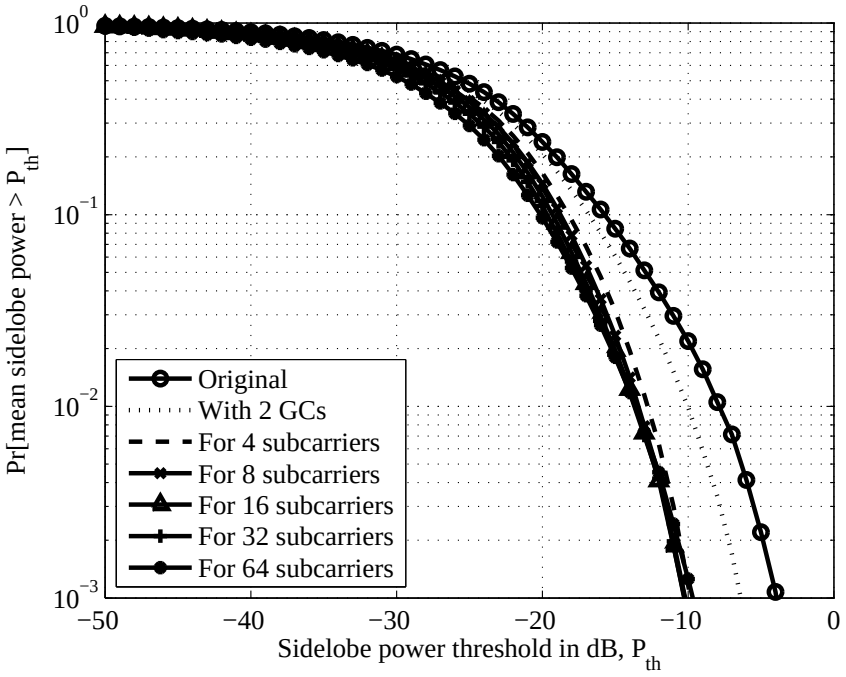

(a) Inserting two CCs

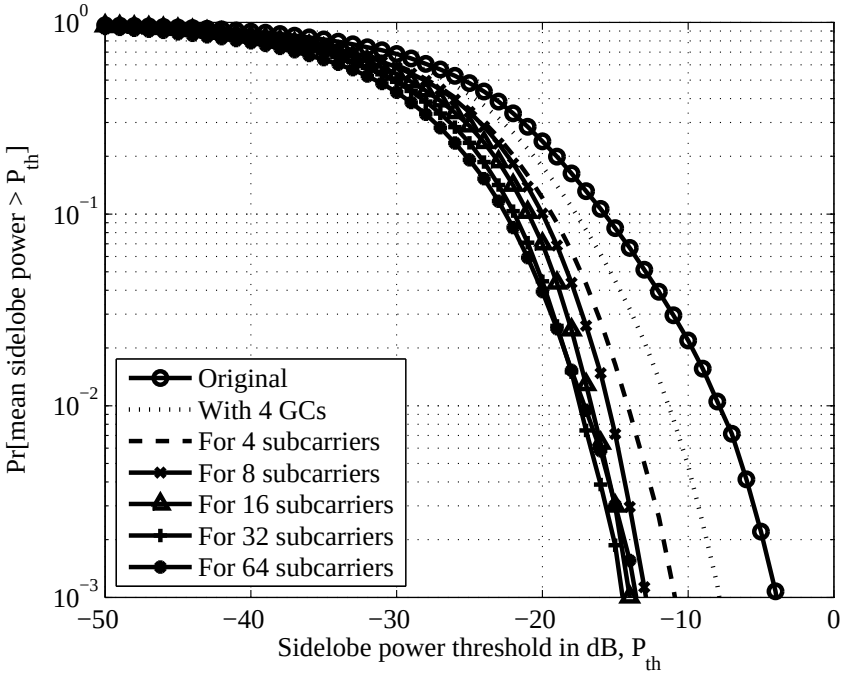

(b) Inserting four CCs

Figure 4.6. Complementary cumulative distribution function (CCDF) with and without inserting cancellation carriers (CCs) in a BPSK-OFDM system.

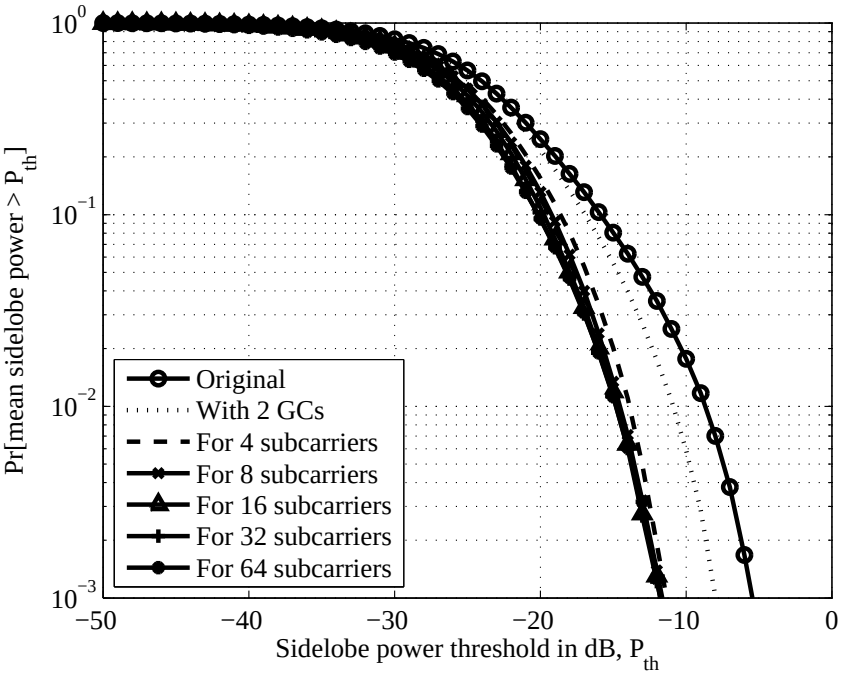

(a) Inserting two CCs

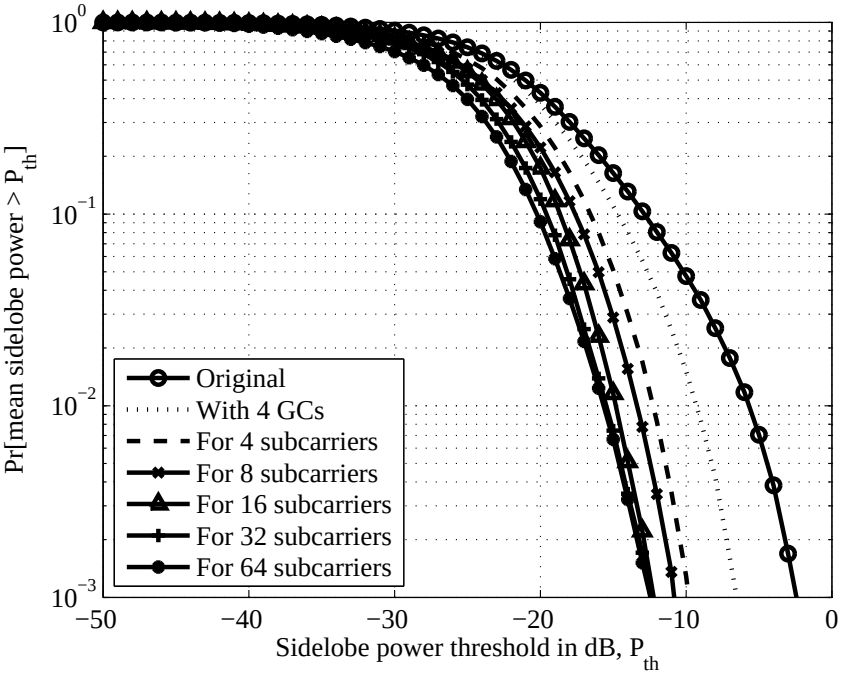

(b) Inserting four CCs

Figure 4.7. Complementary cumulative distribution function (CCDF) with and without inserting cancellation carriers (CCs) in a QPSK-OFDM system.

Figure 4.8(a) shows the interference suppression in a spectrum sharing scenario where the bandwidth between the spectral white spaces, 'a', 'b', 'c' and 'd' is equal. Regions 'a', 'b', 'c' and 'd' have 16, 32, 64 and 128 subcarriers respectively and the regions 'I', 'II', 'III' and 'IV' have 64 subcarriers each. In Figure 4.8(b), the regions I, II, III and IV contain unequal number of subcarriers. It can be seen that even in a spectrum sharing scenario, a clear suppression of the interference levels is achieved. In the case of Region 'III', when the bandwidth between the spectral whitespaces gets shorter as seen from Figure 4.8(b), the sidelobes emerging from the OFDM symbols in those regions do not decay as fast as the case where the bandwidth is larger as in Figure 4.8(a). Even in this case there is a significant amount of suppression by inserting cancellation carriers.

4.1.3.3 Effect on the system

Employing cancellation carriers to suppress the sidelobes has a few adverse effects. However, these are not significant enough to drastically reduce the system performance. For example, in the case of a $N = 64$ subcarrier QPSK-OFDM system employing four cancellation carriers, the situation can be viewed as transmitting the signal over $N = 60$ subcarriers in the original case and over $N = 64$ subcarriers after inserting the CCs. However, this usage of the extra subcarriers has no effect on the PAPR as shown by Figure 4.9.

Similarly, there is not going to be a BER degradation because, the CCs are of the same subcarrier bandwidth as those of the other subcarriers in the system and hence orthogonal. The only main disadvantage of the proposed algorithm is the increase extra transmit energy required to transmit the dummy symbols over the CCs.

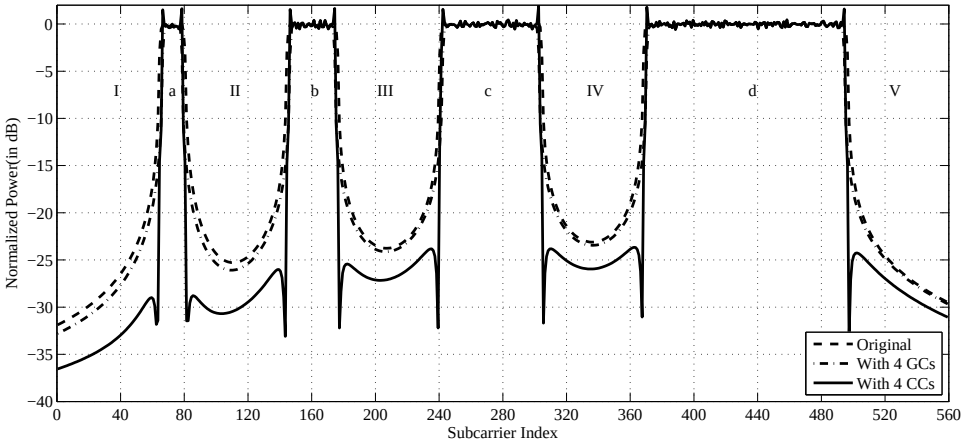

(a) When the bandwidth between the spectral white spaces is equal

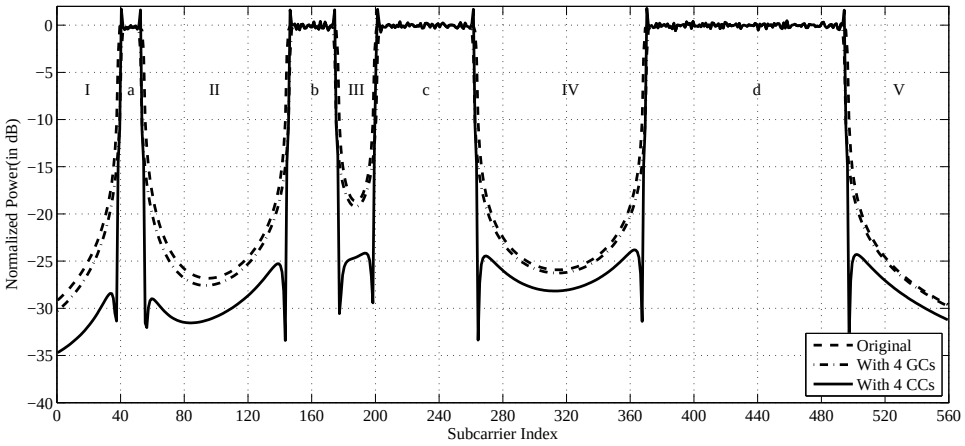

(b) When the bandwidth between the spectral white spaces is unequal

Figure 4.8. An example showing the application of the proposed sidelobe suppression algorithm in a spectrum sharing scenario.

4.2 Proposed Sidelobe Suppression by Constellation Expansion

In this section, a novel algorithm is presented for reducing the interference occurring in OFDM-based cognitive radios caused by the sidelobes of an OFDM symbol. The proposed algorithm exploits the fact that different sequences have

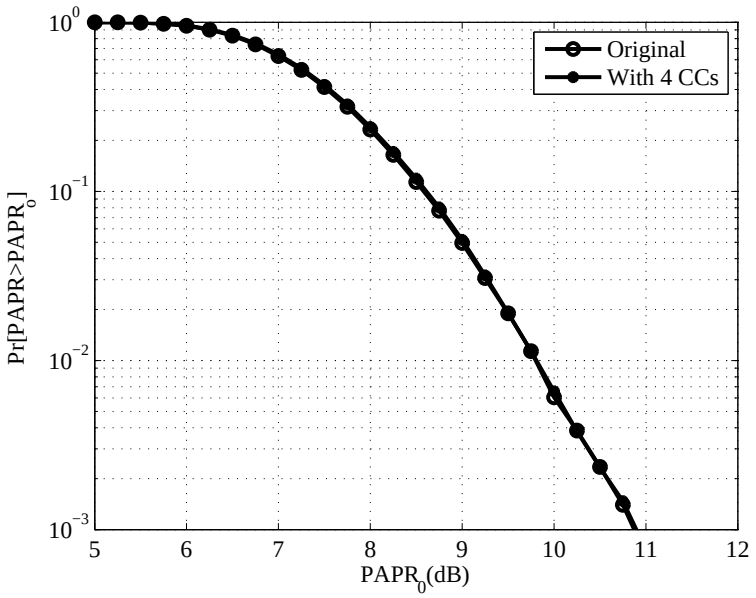

Figure 4.9. Effect of the CCs on the PAPR of N=64 subcarrier QPSK-OFDM system

different sidelobe power levels and hence employs a constellation expansion based iterative approach to achieve a large decrease in the sidelobe power levels. An important advantage of the proposed technique is that there is no side information to be transmitted. The results show that for a wide range of operating conditions, the proposed algorithm achieves a significant suppression in the sidelobe power levels. However, the trade-off involved is a slight increase in the BER which results only because symbols from higher constellation are used to reduce the sidelobe power levels.

4.2.1 Schematic of an OFDM transceiver employing constellation expansion for sidelobe suppression

A general schematic of an OFDM transceiver with dynamic spectrum sensing is shown in Figure 4.10. Without loss of generality, a high speed data stream

is *x(n)* is modulated using M-ary phase shift keying (MPSK). The modulated data stream is then split into N slower data streams using a serial-to-parallel (S/P) converter. The locations of the primary user subcarriers are detected by the dynamic spectrum sensing techniques and the unoccupied bands are used for transmission. The constellation expansion (CE) unit performs the algorithm outlined in the following section to determine the sequence that results in the lowest OOB radiation. The inverse fast fourier transform (IFFT) is then applied to the new sequence. A guard interval with a length greater than the channel delay is added to each OFDM symbol using the cyclic prefix (CP) block to mitigate the effects of intersymbol interference (ISI). Following the parallel-to-serial (P/S) conversion, the baseband OFDM signal *s(n)* is then passed through the transmitter's radio frequency (RF) chain, to amplify the signal and upconvert it to the desired frequency.

The receiver performs the reverse operation of the transmitter, mixing the RF signal to baseband and yielding *r(n)*. After converting the signal to parallel streams using S/P converter, the cyclic prefix is discarded and the fast fourier transform is applied to transform the time domain data into frequency domain. After compensating for distortion introduced by the channel using equalization, the data in the subcarriers is multiplexed using a P/S converter, and demodulated into a reconstructed version of the original high-speed input, $\hat{x}(n)$.

4.2.2 Proposed CE-based sidelobe suppression technique

In the proposed technique, the symbols of a modulation scheme that modulates k bits/symbol and consisting of 2^k constellation points are mapped to a modulation scheme that modulates *(k+1)* bits/symbol and consisting of 2^{k+1} con-

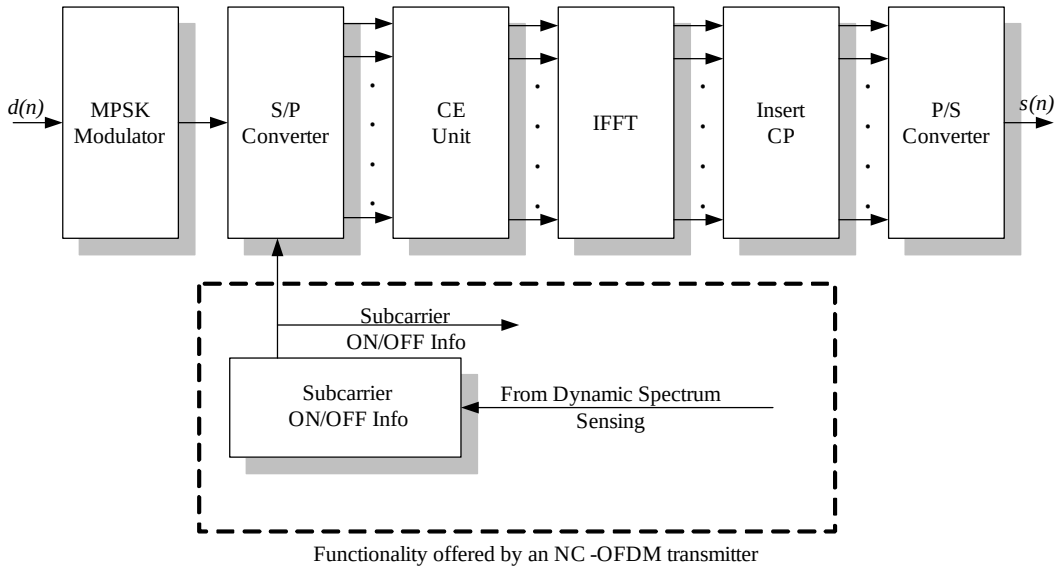

(a) An OFDM-based transmitter employing the CE technique

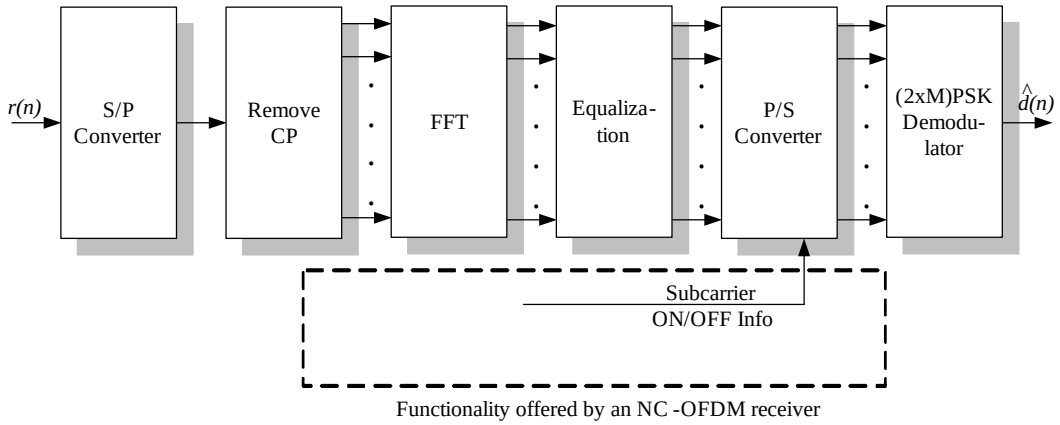

(b) An OFDM-based receiver employing the CE technique

Figure 4.10. Schematic of an OFDM-based cognitive radio transceiver employing the proposed CE-based sidelobe suppression technique.

stellation points. In other words, for every constellation point in the original symbol sequence, there are two points to choose from, in the expanded constellation space. Selecting one of the points on a random basis, each symbol in a sequence of N symbols is mapped to N symbols from the expanded symbol set. An underlying assumption in the proposed technique is, the transmitter and the receiver are assumed to have the knowledge of the points of the expanded constellation that are associated with the points in the original constellation. Hence, after the demodulation process, the symbols can be re-mapped to the points of the original constellation. With this knowledge, no side information is needed to be shared between the transmitter and the receiver.

As an example, two ways of mapping BPSK symbols to QPSK symbols and from QPSK symbols to 8-PSK symbols are shown in Figure 4.11 and Figure 4.12 respectively. The logic behind this association of points from a lower constellation to a higher constellation is to take advantage of the randomness involved in selecting one of the two points and hence the combination of different in-phase and quadrature-phase components from all the subcarriers would result in a sequence with the lowest sidelobes.

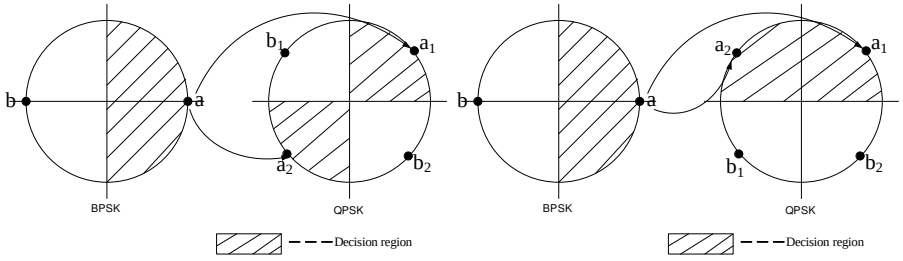

(a) Mapping I (b) Mapping II

Figure 4.11. Two ways of mapping symbols from BPSK constellation to QPSK

The iterative algorithm that selects the sequence randomly is shown in Fig-

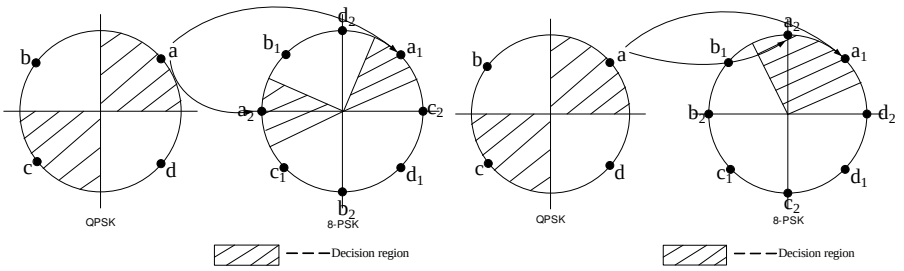

(a) Mapping I (b) Mapping II

Figure 4.12. Two ways of mapping symbols from QPSK constellation to 8PSK

ure 4.13. In this algorithm, the variable *interference_threshold* is only intended to break the iterative process in the probabilistically least likely occurrence of finding a sequence with the sidelobes that are at a low value, in which case further iterations[1]are unnecessary. It can be noticed from the algorithm that, the complexity of the algorithm is directly dependant on the value of *iterations_threshold*, i.e., the maximum number of iterations allowed. If the value of this variable is large, there is a greater number of sequences from which the desired sequence with the lowest maximum sidelobe power is chosen. Thus, there is a greater probability of finding a sequence which has lower sidelobe power levels. Therefore, the average suppression over a large number of symbols can be expected to be lower in the case where the number of allowed iterations is large.

A similar technique based on expanding the signal constellation has been proposed in [34, 35] for PAPR reduction. However, the similarity between the proposed technique and these techniques in finding the desired sequence ends there. [34] proposes an optimization algorithm and [35] relies on a complex search technique, to find the desired sequence, whereas the proposed technique relies on

[1]Here, iteration means the number of samples out of a sample space containing 2^N points. That is, in the case of a N-subcarrier system, there are 2^N ways of associating the symbol sequence from the original constellation to the higher order constellation.

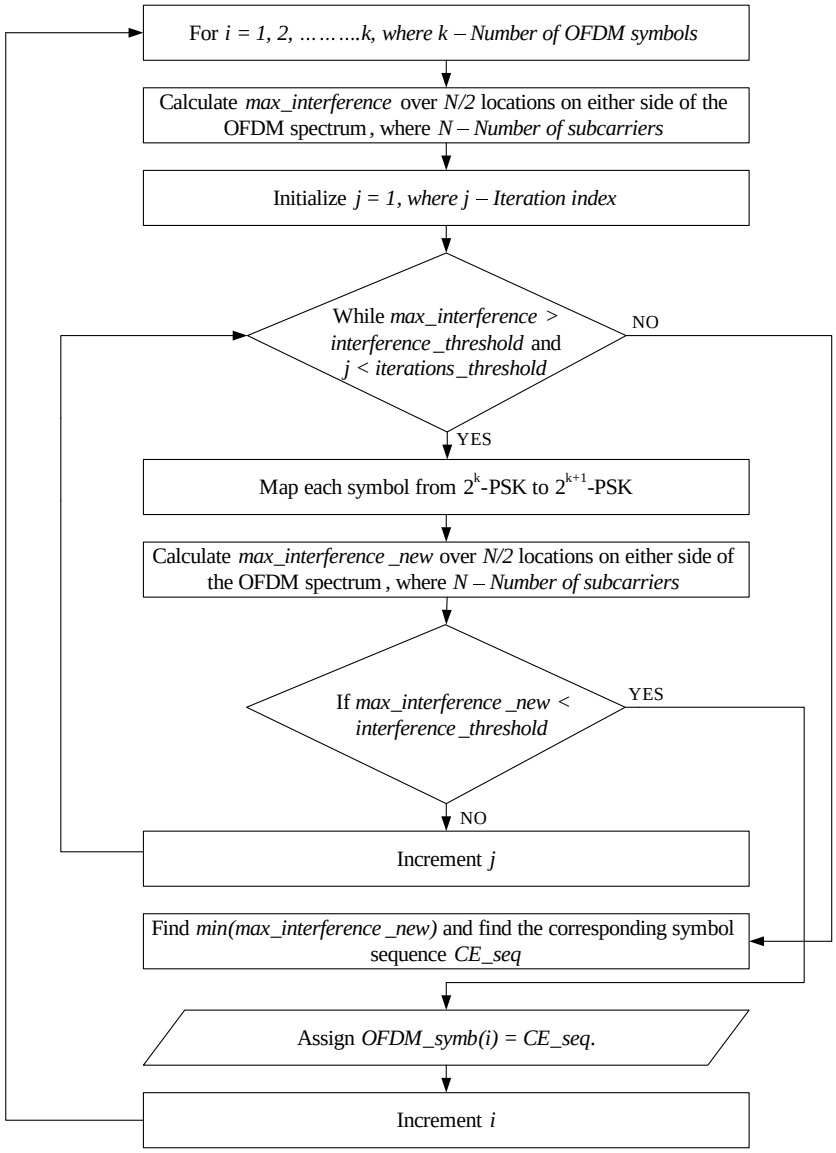

Figure 4.13. An iterative algorithm for symbol selection using constellation expansion

the iterative algorithm shown in Figure 4.13.

4.2.3 Simulation Results

The proof of the effectiveness of the proposed algorithm is presented in this subsection.

4.2.3.1 Simulation Parameters

An $N = 16$ subcarrier system and an $N = 64$ subcarrier system modulated by BPSK and QPSK is considered. The expanded constellations considered for these two cases are QPSK and 8-PSK respectively. The parameter *iterations_threshold* is set to 64. Two different sets of mapping are considered and the trend in sidelobe suppression is studied. Furthermore, the impact of the parameter *iterations_threshold*, i.e., the maximum allowed number of iterations and the proper selection of the symbols from the higher constellation set on the interference suppression is studied. Finally, the constellation expansion approach is applied to a spectrum sharing scenario containing five channels, with the secondary user occupying two channels. In all the cases, normalized power spectrum plots averaged over 50000 OFDM symbols and complementary cumulative distribution functions (CCDFs) are presented to illustrate the effectiveness of the proposed algorithm.

4.2.3.2 Results

In Figure 4.14, the averaged power spectrum plot and the CCDF plot of the sidelobe power of a 16 subcarrier BPSK-modulated OFDM system expanded to QPSK is shown. A suppression of 10 dB is observed from Figure 4.14 (a). The CCDF plot also shows the suppression achieved in sidelobe levels. For example,

the 0.1% sidelobe power is suppressed by just over 10 dB from the original case.

Figure 4.15 shows a similar trend in the suppression of sidelobe levels by applying constellation expansion for a QPSK-OFDM modulated system. The normalized power spectrum plot and the CCDF plot of the sidelobe power for QPSK-OFDM expanded to 8PSK are shown in Figures 4.15 (a) and (b) respectively. From Figure 4.15(a), it can be seen that the suppression of the peak interference causing sidelobe is around 10.3 dB. Also, there is a marked reduction in the 0.1% of sidelobe power. In other words, in the original case 99.9% of the sidelobe power is below $-5dB$ whereas, after applying constellation expansion, 99.9% of the sidelobe power is below $-15dB$. The maximum allowed number of iterations used in generating these plots is 64.

Figure 4.16 shows the CCDF plot of the sidelobe power for a QPSK-OFDM transceiver system expanded to 8PSK for various number of iterations. This plot shows a trend of how the increase in the number of iterations has an effect on the sidelobe suppression characteristics. It can be noted from this figure that, as the number of maximum allowed iterations increases, the sidelobe suppression characteristics improve. However, the improvement is noticeable when the value of *iterations_threshold* is increased from 8 to 64, but when increased from 64 to 256, the improvement in sidelobe suppression is not commensurate with the increase in the number of iterations. Therefore, choosing a maximum allowed number of iterations of 64 is a reasonable option to balance the trade-off in the increase of the number of computations and the improvement in the sidelobe reduction characteristics. The reason why there is an improvement in the sidelobe suppression characteristics with increase in the number of iterations is because, as the number of iterations increases, the algorithm is able to search from a greater number of se-

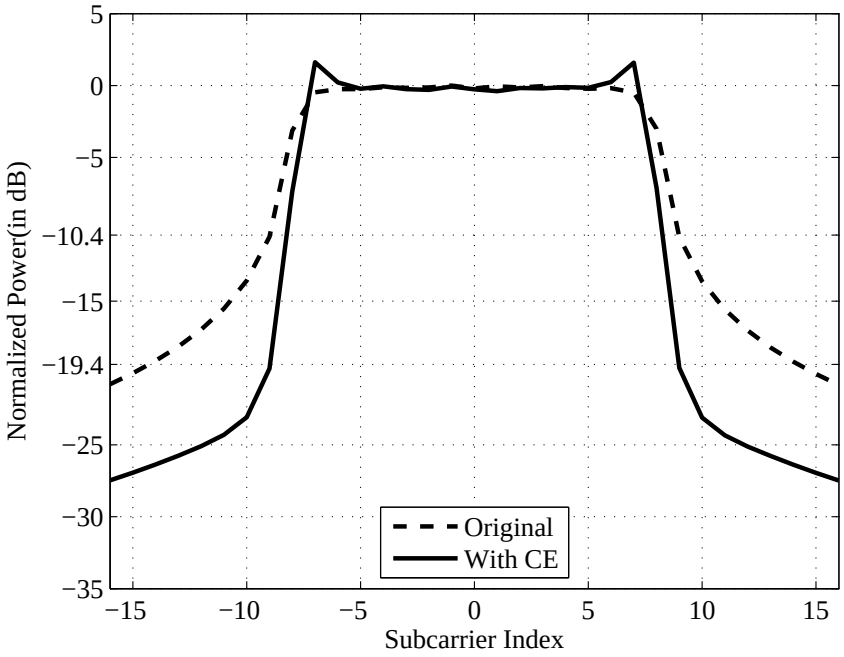

(a) Normalized power spectrum for BPSK-modulated OFDM and its expanded QPSK modulated OFDM

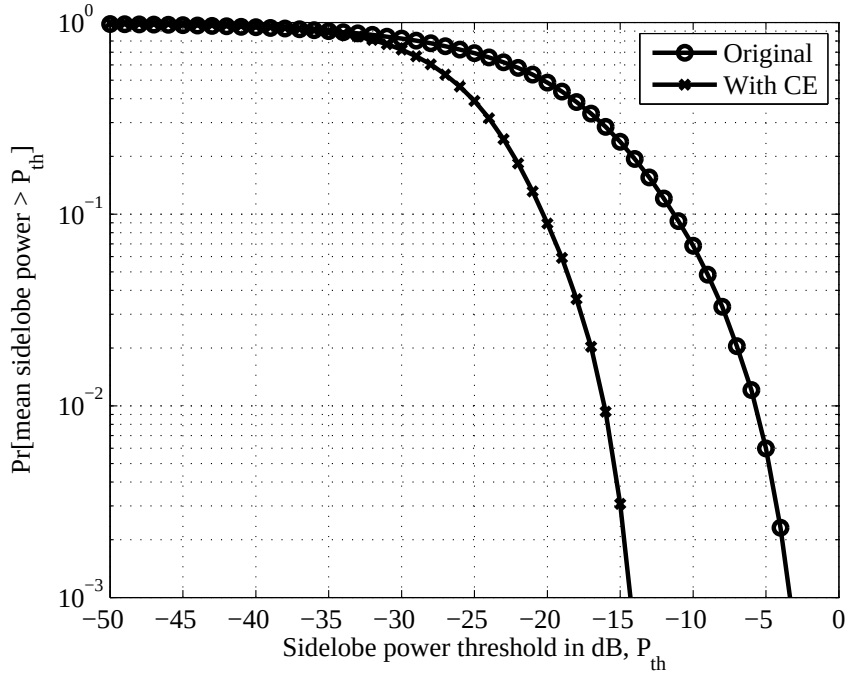

(b) CCDF of sidelobe power for BPSK-modulated OFDM and its expanded QPSK modulated OFDM

Figure 4.14. Sidelobe levels of a BPSK-OFDM system with and without constellation expansion

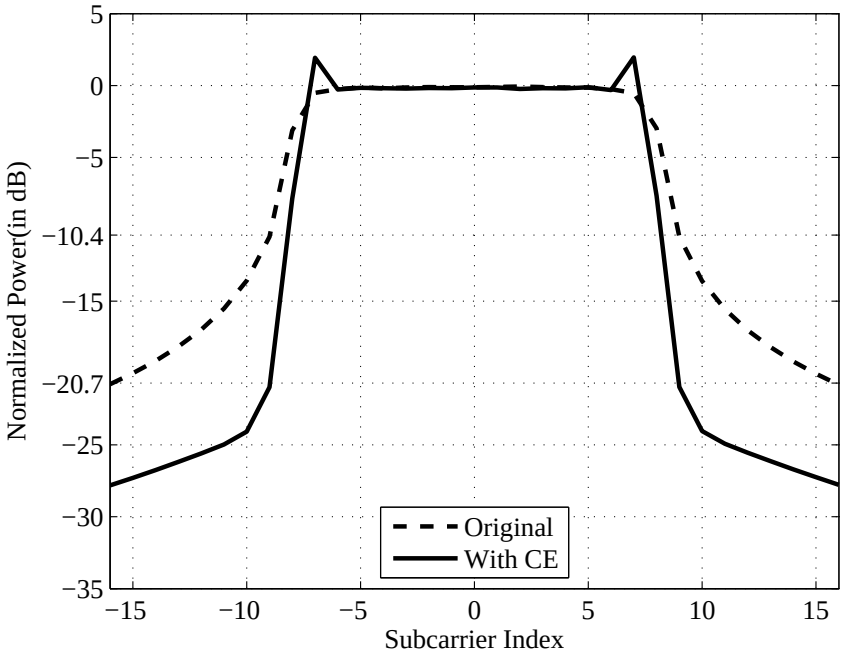

(a) Normalized power spectrum for QPSK-modulated OFDM and its expanded 8-PSK modulated OFDM

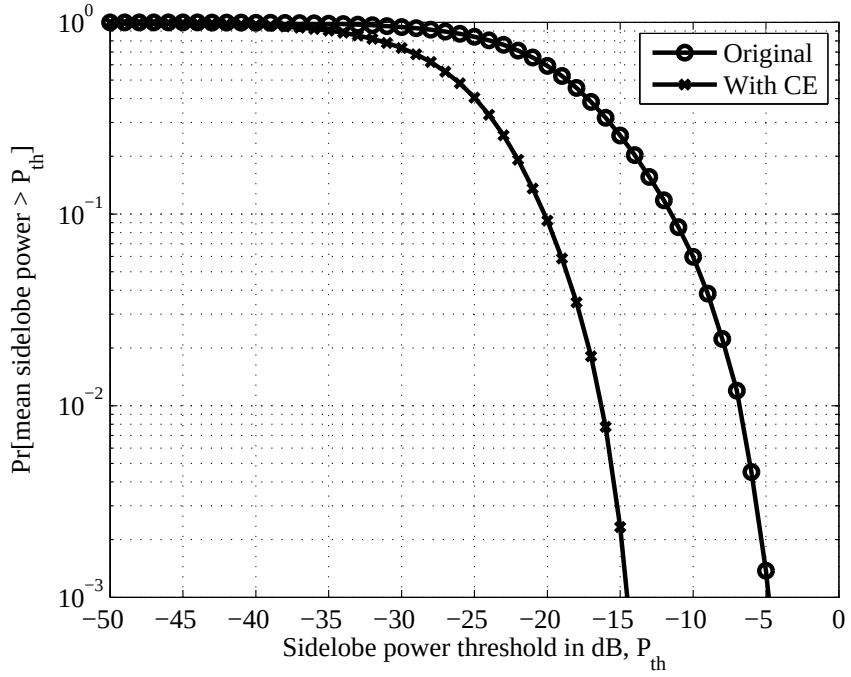

(b) CCDF of sidelobe power for QPSK-modulated OFDM and its expanded 8-PSK modulated OFDM

Figure 4.15. Sidelobe levels of a QPSK-OFDM system with and without constellation expansion

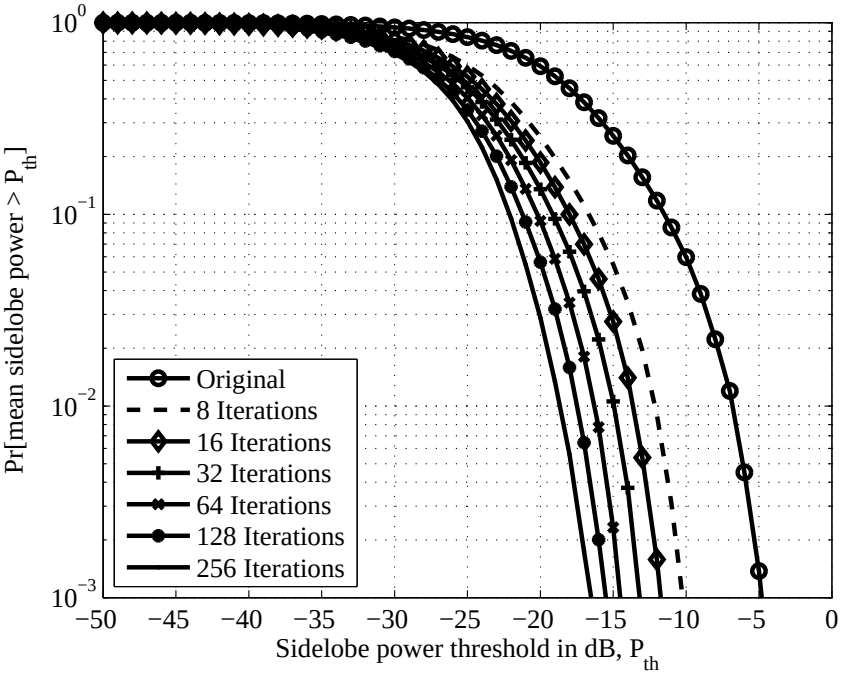

Figure 4.16. CCDF of sidelobe power for QPSK-modulated OFDM and its expanded 8-PSK modulated OFDM for different number of iterations

quences for the one with the least $max\_interference\_new$. Hence, when averaged over a large number of OFDM symbols, an improvement is observed.

Another interesting test case would be the proper selection of the symbol set from the higher constellation diagram that need to be mapped to the symbols of the original constellation. As explained in the previous section, the idea of using symbols from the higher constellation diagram is to take advantage of the randomness involved and hence select a sequence iteratively so that it has the lowest sidelobe levels. From Figure 4.11(a), point a is mapped to points a_1 and a_2. Instead, if the mapping shown in Figure 4.11(b) is implemented, a random selection of the one point would lead to selecting points which have either the same real component or the same imaginary component. Thus, there might not be any difference in the sidelobe pattern over one degree of freedom except for

a change in scale. However, associating points as shown in Figure 4.11(a) would allow a greater degree of randomness in the selection process as both the real and imaginary components are 180^o out-of-phase. This is illustrated by the plot shown in Figure 4.17. The effects of not choosing the correct mapping is clearly seen from this plot.

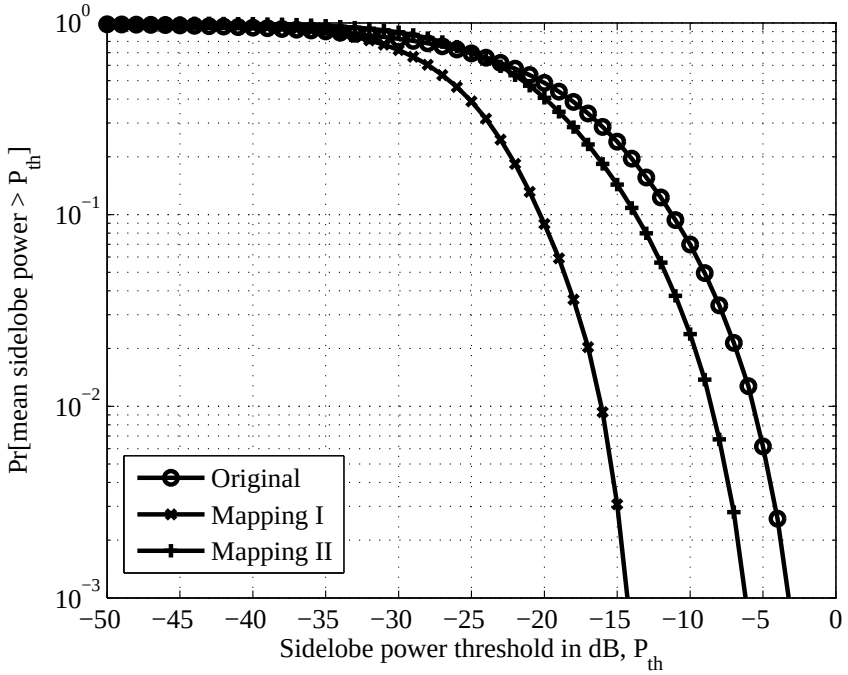

Figure 4.17. CCDFs of sidelobe power for BPSK-modulated OFDM and its expanded QPSK modulated OFDM for different mappings

It can be noted from Figures 4.11(a) and **??** (a) that the decision region decreases as a result of constellation expansion and hence a degradation of bit error rate (BER) is expected.

The proposed technique of constellation expansion when applied to a system with 64 subcarriers, the results shown in Figures 4.18 and 4.19. A similar trend in the suppression of the sidelobes is observed.

Finally, Figure 4.20 shows the interference suppression in the spectrum sharing

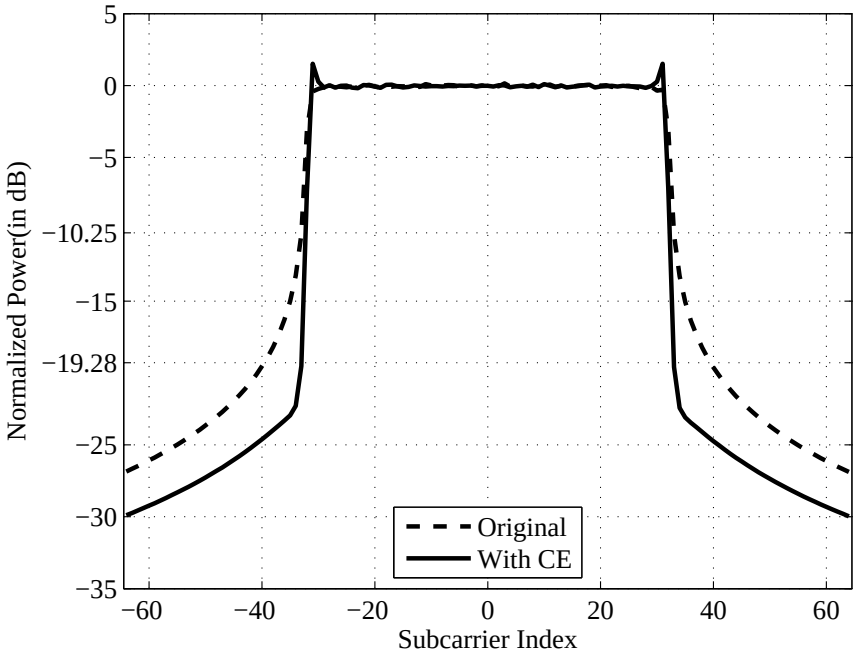

(a) Normalized power spectrum for BPSK-modulated OFDM and its expanded QPSK modulated OFDM

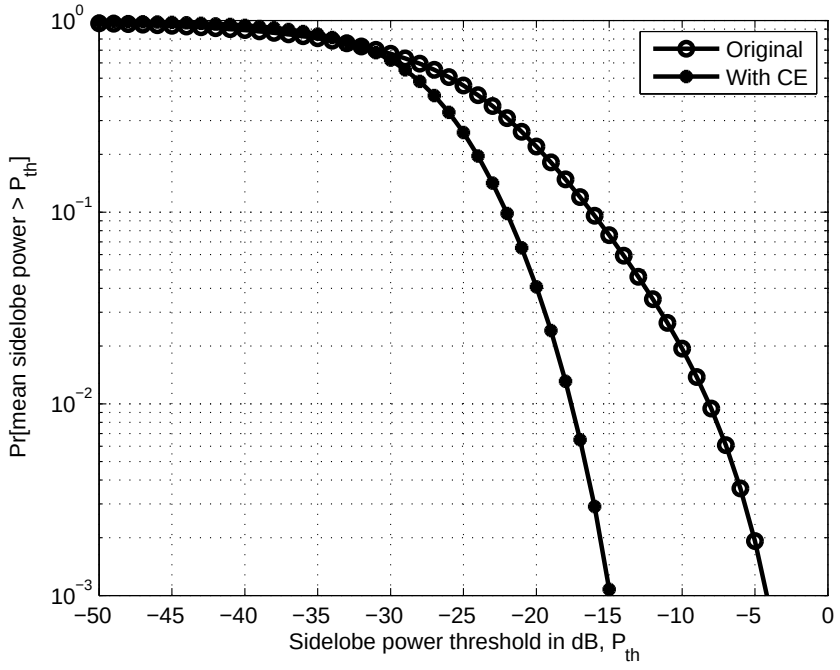

(b) CCDF of sidelobe power for BPSK-modulated OFDM and its expanded QPSK modulated OFDM

Figure 4.18. Sidelobe levels of a BPSK-OFDM system with and without constellation expansion

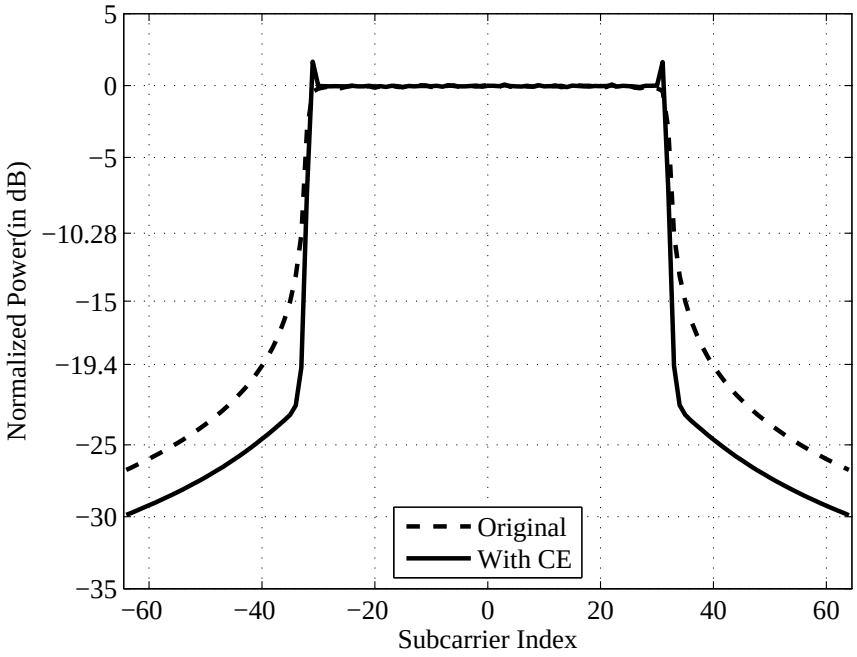

(a) Normalized power spectrum for QPSK-modulated OFDM and its expanded 8-PSK modulated OFDM

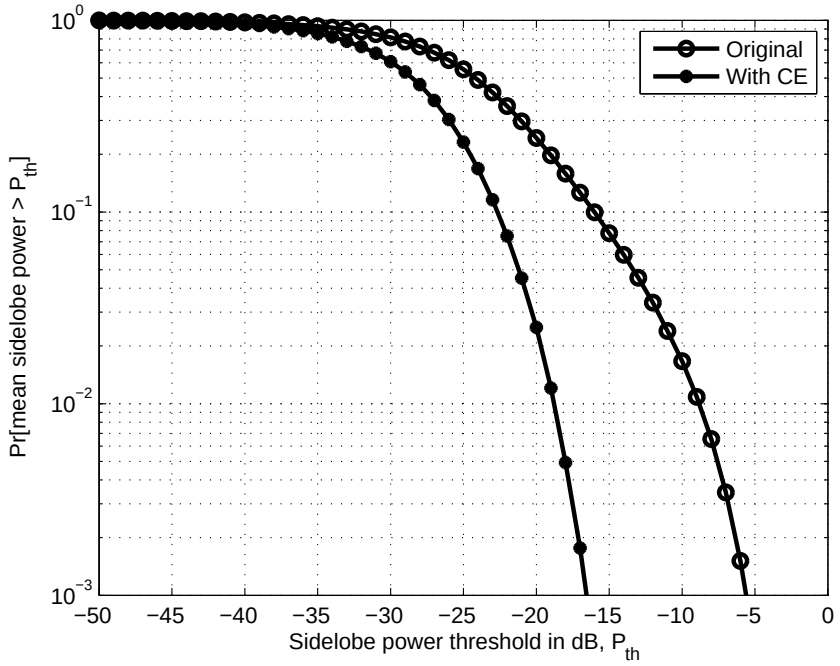

(b) CCDF of sidelobe power for QPSK-modulated OFDM and its expanded 8-PSK modulated OFDM

Figure 4.19. Sidelobe levels of a QPSK-OFDM system with and without constellation expansion

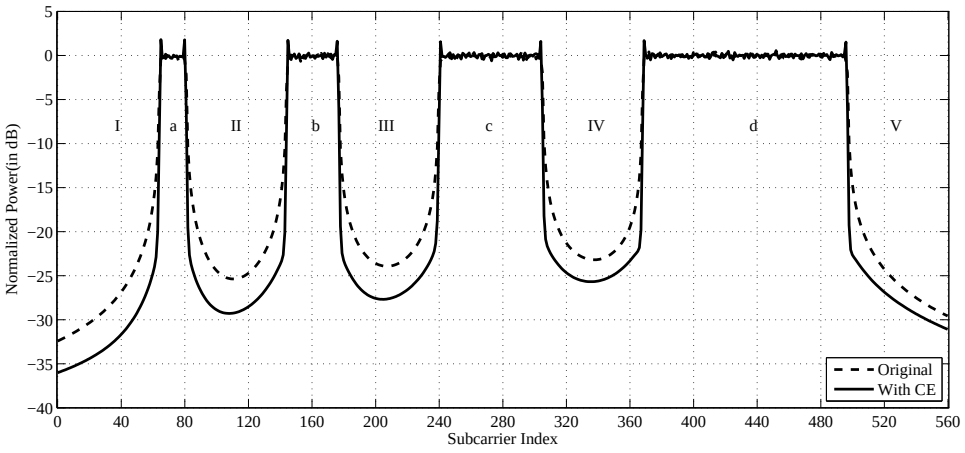

(a) When the bandwidth between the spectral white spaces is equal

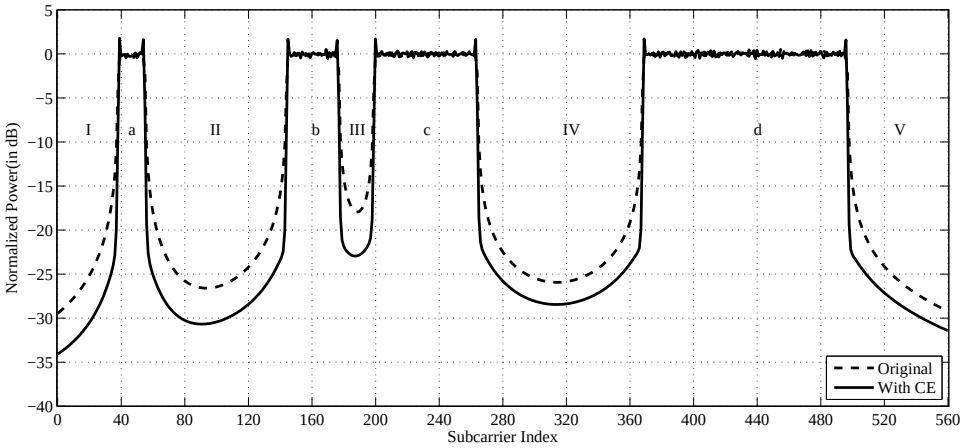

(b) When the bandwidth between the spectral white spaces is unequal

Figure 4.20. An example showing the application of the proposed sidelobe suppression algorithm in a spectrum sharing scenario.

scenario considered in the previous section. Figure 4.20(a) shows the interference suppression in the scenario where, the bandwidth between the spectral white spaces, 'a', 'b', 'c' and 'd' is equal. Regions 'a', 'b', 'c' and 'd' have 16, 32, 64 and 128 subcarriers respectively and the regions 'I', 'II', 'III' and 'IV' have 64 subcarriers each. In Figure 4.20(b) the regions I, II, III and IV contain unequal number of subcarriers. Again, it can be seen that, even in a spectrum sharing scenario, a clear suppression of the interference levels is achieved. In the case of

region 'III', when the bandwidth between the spectral whitespaces gets shorter as seen from Figure 4.20(b), the sidelobes emerging from the OFDM symbols in those regions do not decay as fast as the case where the bandwidth is larger as in Figure 4.20(a). Even in this case there is a significant amount of suppression by employing constellation expansion.

4.2.3.3 Effect on the system

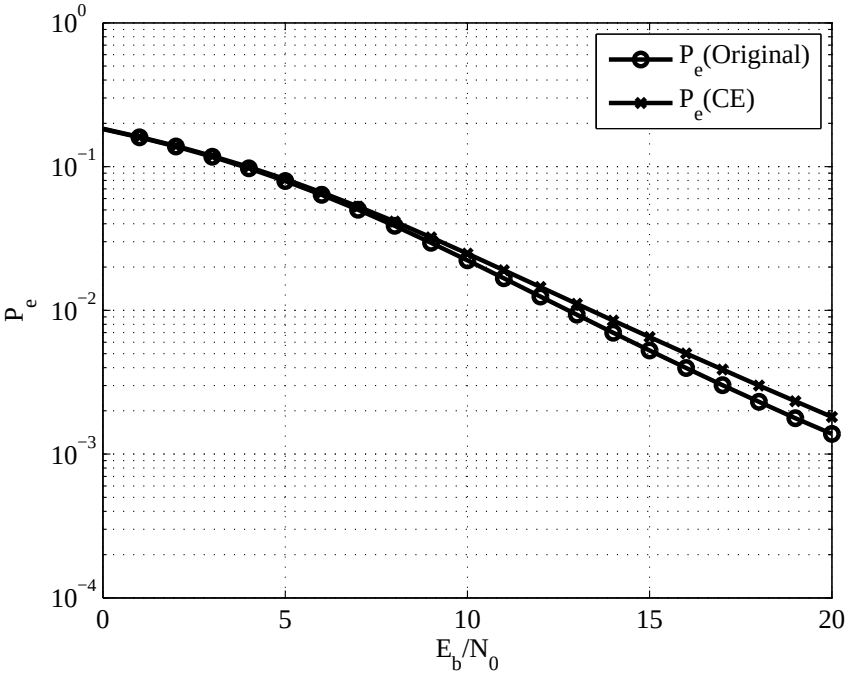

Figure 4.21. BER of a N=16 subcarrier QPSK-modulated OFDM and its expanded 8-PSK modulated OFDM

BER degradation : The technique proposed in the this section uses symbols from the higher order constellation diagram. Therefore, a degradation in the BER is expected. However, after mapping the symbols back to the original constellation, it can be seen from the BER plot of a $N = 16$ subcarrier QPSK-OFDM

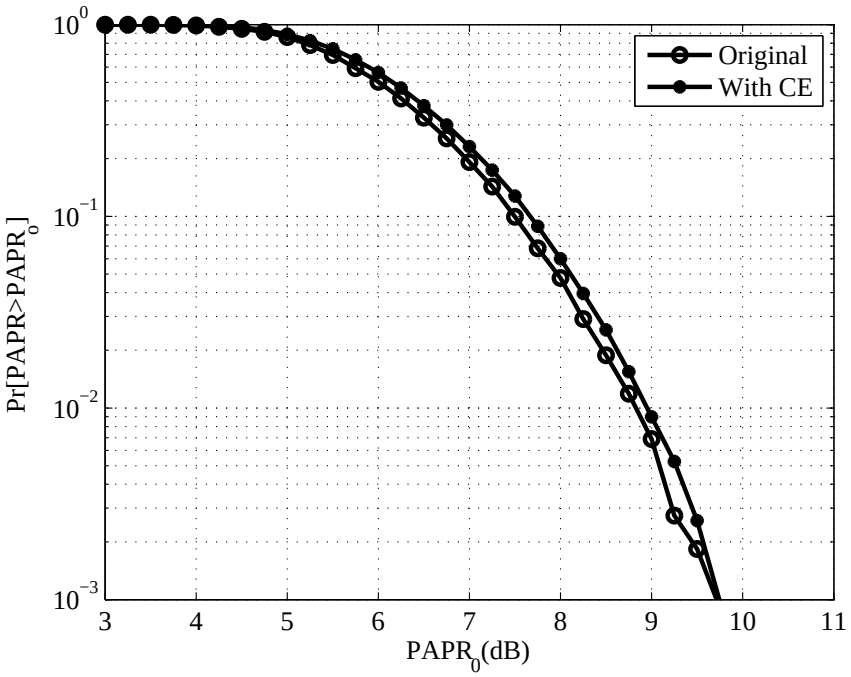

Figure 4.22. PAPR plot of a N=16 subcarrier QPSK-modulated OFDM and its expanded 8-PSK modulated OFDM

system shown in Figure 4.21 that, the degradation is not substantial enough to drastically lower the system performance. The channel model used in generating this plot is a five-tap Rayleigh with the tap gains being [1/2 1/4 1/6 1/20 1/30]. Also, perfect channel estimation is assumed at the receiver.

PAPR degradation : As the symbols from the higher order constellation diagram are used to transmit the symbols from the original constellation, a slight degradation in the PAPR is also expected. As shown in Figure 4.22, 0.1% of the PAPR in the case of a N=16 subcarrier QPSK-modulated OFDM, increases by less than $0.1dB$. Thus, the PAPR characteristic doesn't worsen significantly by applying the constellation expansion technique, even though symbols from the higher order constellation diagram are used in order to achieve sidelobe suppression.

Chapter 5

Conclusion

In this thesis, an attempt has been made at suppressing the interference power resulting from the rental system to the legacy system to acceptable levels. Consequently, the coexistence of the legacy and the rental systems, is made more feasible. The two novel algorithms that have been proposed in this thesis are:

- A cancellation subcarrier based sidelobe suppression technique which, calculates the interference levels algebraically and inserts cancellation carriers based on the interference levels.
- A constellation expansion based approach wherein, the symbols of the original constellation are expanded to symbols from the higher constellation diagram and the sequence with the lowest sidelobe power levels is chosen iteratively.

As a result of this research, two peer-reviewed publications have been produced:

- Rakesh Rajbanshi, Srikanth Pagadarai, Alexander M. Wyglinski, and Gary J. Minden. *Sidelobe Suppression Technique for OFDM-based Cognitive Ra-*

dios. Submitted to the EURASIP Journal on Wireless Communications and Networking – Special Issue on Cognitive Radio and Dynamic Spectrum Sharing Systems, June 2007.

- Srikanth Pagadarai, Rakesh Rajbanshi, Alexander M. Wyglinski, and Gary J. Minden. *A constellation expansion approach for sidelobe suppression in OFDM systems*. In preperation for the IEEE Wireless Communications and Networking Conference (WCNC), September 2007.

5.1 Future Work

There exist a number of areas for future work related to what has been presented in this thesis.

- The insertion of cancellation carriers concept for sidelobe suppression can be developed to design an adaptive algorithm that decides on the number of subcarriers to use for sidelobe suppression depending on the desired interference suppression. However, this would require sending side information to the receiver about the particular number of subcarriers used in each band.

- The existing algorithms including those presented in this thesis do not utilize the statistical relationship between the random symbols carried by the subcarriers and the resulting sidelobe power levels. An understanding of such a relationship would greatly help in designing better techniques with better sidelobe suppression.

- Also, it would be interesting to the proposed algorithms implemented on a cognitive/software-defined radio hardware platform.

- A sidelobe-suppression technique based on varying the data-rates of the subcarriers that are closer to the edges of the OFDM spectrum can be developed. The premise of this algorithm is, if the subcarriers that are closer to the edges of the OFDM spectrum have slower data rates, then the subcarrier bandwidth would be smaller and the sidelobes emerging from them would also be smaller, leading to low sidelobe power levels.

References

[1] Federal Communications Commission, "Spectrum policy task force report." EE Docket No. 02-135, 2002.

[2] R. Rajbanshi, *OFDM-based cognitive radio for DSA networks.* Ph.d dissertation, University of Kansas, Lawrence, KS, USA, May 2007.

[3] T. A. Weiss and F. K. Jondral, "Spectrum pooling: an innovative strategy for the enhancement of spectrum efficiency," *IEEE Commun. Mag.*, vol. 43, pp. 8–14, March 2004.

[4] J. Mitola III, "Cognitive radio for flexible mobile multimedia communications," in *Proc. IEEE Int. Wksp. Mobile Multimedia Commun.*, vol. 1, (San Diego, CA, USA), pp. 3–10, Nov. 1999.

[5] R. Prasad, *OFDM for Wireless Communication Systems.* Artech House Inc., 2004.

[6] R. Rajbanshi, A. M. Wyglinski, and G. J. Minden, "An efficient implementation of the NC-OFDM transceivers for cognitive radios," in *Proc. IEEE Int. Conf. on Cognitive Radio Oriented Wireless Networks Commn.*, (Mykonos, Greece), June 2006.

[7] T. A. Weiss, J. Hillenbrand, A. Krohn and F. K. Jondral, "Mutual interference in OFDM-based spectrum pooling systems," in *Proc. IEEE Veh. Technol. Conf. - Fall*, vol. 4, pp. 1872–1877, May 2004.

[8] S. Kapoor and S. Nedic, "Interference suppression in DMT receivers using windowing," in *Proc. IEEE Int. Conf. on Commun.*, vol. 2, (New Orleans, LA, USA), pp. 778–782, June 2000.

[9] S. Brandes, I. Cosovic, and M. Schnell, "Sidelobe supression in OFDM systems by insertion of cancellation carriers," in *Proc. 62nd IEEE Veh. Technol. Conf. - Fall*, vol. 1, pp. 152–156, Sept. 2005.

[10] I. Cosovic, S. Brandes, and M. Schnell, "Subcarrier weighting: A method for sidelobe suppression in OFDM systems," *IEEE Commn. Letters*, vol. 10, No. 6, June 2006.

[11] I. Cosovic and T. Mazzoni, "Suppression of sidelobes in OFDM systems by multiple choice sequences," *European Trans. Commun.*, vol. 1, pp. 623–630, Dec. 2006.

[12] J. Mitola III, "Software Radio Architecture: A Mathematical Perspective," in *Proc. IEEE Journal on selected areas in Commn.*, vol. 17, No. 4, April 1999.

[13] D. Čabrić and R. W. Brodersen, "Physical layer design issues unique to cognitive radio systems," *IEEE 16th International Symposium on Personal, Indoor and Mobile Radio Commun.*, vol. 2, pp. 759–763, Sept. 2005.

[14] D. Čabrić, D. O'Donnel, M. S. W. Chen and R. W. Brodersen, "Spectrum sharing radios," *IEEE Commun. Mag.*, vol. 2, pp. 30–45, 2006.

[15] J. Mitola, III, *Cognitive Radio Architecture*. New Jersey, USA: A John Wiley and Sons, Inc., 2006.

[16] R. Rajbanshi, A. M. Wyglinski, and G. J. Minden, *Cognitive Radio Communication Networks*, ch. 5. Springer-Verlag, 2007.

[17] S. B. Weinstein and P. M. Ebert, "Data transmission by frequency division multiplexing using the discrete fourier transform," *IEEE Trans. Commun. Technol.*, vol. 19, pp. 628–634, Oct 1971.

[18] R. R. Mosier and R. G. Clabaugh, "Kineplex, a bandwidth efficient binary transmission system," *AIEE Trans.*, vol. 76, pp. 723–728, Jan 1958.

[19] B. R. Salzberg, "Performance of an efficient parallel data transmission system," *IEEE Trans. Commun.*, vol. 15, pp. 805–813, Dec 1967.

[20] B. Hirosaki, "An orthogonally multiplexed QAM system using the discrete fourier transform," *IEEE Trans. Commun.*, vol. 29, pp. 982–989, July 1981.

[21] J. G. Proakis and D. K. Manolakis, *Digital Signal Processing: Principles, Algorithms and Applications*. Upper Saddle River, NJ, USA: Prentice Hall, 1995.

[22] A. Peled and A. Ruiz, "Frequency domain data transmission using reduced computational complexity algorithms," *Proc. of the IEEE Intl. Conf. on Acoustics, Speech, and Signal Processing*, pp. 964–967, 1980.

[23] T. S. Rappaport, *Wireless Communication: Principles and Practice*. Upper Saddle River, NJ, USA: Prentice Hall, 2006.

[24] S. K. Shanmugan and A. M. Breipohl, *Random Signals: Detection Estimation and Data Analysis*. USA: John Wiley & Sons, 1988.

[25] J. J. van de Beek, P. Ödling, S. K. Wilson and P. O. Börjesson, "Orthogonal frequency division multiplexing." URSI, Wiley, 1999:2002.

[26] A. M. Wyglinski, *Physical layer loading algorithms for indoor wireless multicarrier systems*. Ph.d dissertation, McGill University, Montreal, Quebec, Canada, Nov. 2004.

[27] H. Schulze and C. Lüders, *Theory and applications of OFDM and CDMA: Wideband Wireless Communications*. A John Wiley and Sons, Inc., 2005.

[28] N. Y. Ermolova and P. Vainikainen, "On the relationship between peak factor of a multicarrier signal and aperiodic correlation of the generating sequence," *IEEE Commn. Letters*, vol. 7, pp. 107–108, March 2003.

[29] J. G. Proakis, *Digital Communications*. New York, NY, USA: McGraw Hill, 2001.

[30] IEEE802.11a, "Wireless LAN Medium Access Control (MAC) and Physical Layer (PHY) Specifications: High-speed Physical Layer in the 5 GHz band." IEEE, Tech. Rep., 1999.

[31] ETSI-TS-101475, "Broadband Radio Access Networks (BRAN); HIPERLAN Type 2; Physical (PHY) Layer." ETSI, Tech. Rep., 2001.

[32] A. D. S. Jayalath and C. Tellambura, *Interleaved PC-OFDM to Reduce Peak-to-Average Power Ratio*, vol. 703 of *Springer International Series in Engineering and Computer Science*, pp. 239–250. Netherlands: Springer, 2002.

[33] I. Cosovic, S. Brandes, and M. Schnell, "Physical layer design challenges of an OFDM based overlay system," *IST Mobile & Wireless Commun. summit*, June 2006.

[34] C. E. Tan, and I. J. Wassell, "Data bearing peak reduction carriers for OFDM systems," in *Proc. IEEE Infor. Commun. and Sig. Proc., 2003 and the Fourth Pacific Rim Conference on Multimedia*, vol. 2, pp. 854–858, Dec. 2003.

[35] Seung Hee Han and Jae Hong Lee, "Peak-to-average power ratio reduction of an OFDM signal by signal set expansion," in *Proc. IEEE Int. Conf. Commun.*, vol. 2, pp. 867–871, June 2004.